SOCIETY OF ACTUARIES

Modeling and Forecasting Cause-of-Death Mortality

December 2019

Modeling and Forecasting Cause-of-Death Mortality

AUTHORS

Alexandre Boumezoued
Jean-Baptiste Coulomb
Al Klein
Damien Louvet
Eve Titon

SPONSORS

Product Development Section
Financial Reporting Section
Modeling Section
Committee on Life Insurance Research

CONTENTS

Modeling and Forecasting Cause-of-Death Mortality

Section 1: Introduction

To date, aggregate mortality tables of general populations have been used for providing both historical mortality analysis and future scenarios based on appropriate forecasting tools. For such data, the Human Mortality Database (HMD) has become one of the primary reference providers of mortality estimates since its launch in 2002.

In February 2017, the Society of Actuaries (SOA) provided support to HMD to expand the database by including cause of death information for a set of countries. Beyond the World Health Organization data by causes of deaths, the release of more homogeneous and user-friendly data on cause-of-death mortality rates, therefore, opens the way for the profession to analyze and measure mortality and longevity risks at a more granular level.

On this basis, this project aims at going beyond historical analysis by providing coherent and consistent future forecasts of cause-specific death rates, allowing the practitioner to:

- Understand the interaction and joint dynamics of the causes of death on granular death rates;
- Anticipate short- and medium-term evolution of the relative importance of death-related pathologies in future years;
- Measure the longevity and mortality risk as a result of the decrease or increase in mortality due to specific causes;
- Refine and challenge classical projections based on aggregate (all-cause) information
- Understand the key drivers of future aggregate mortality dynamics.

One of the key objectives of this project is to provide a unified source for cause-of death projections. The resulting projections could be used to compare against experts' opinions on advancements and deteriorations in mortality that may be country-specific or cause of death related.

The focus of this report is United States mortality, although the methodology described is general and could be extended to other countries.

This report is organized as follows:

- Section 3:, contains a detailed definition of cause-of-death rates, as well as a description of supporting data used in the project.
- Section 4: analyzes the historical pattern of U.S. mortality by cause of death according to the classification chosen in this project.
- Section 5:discusses the modeling framework used.
- Section 6:contains the forecasting outputs, as well as a comparison to the all-cause projection.
- Finally, appendices and References are detailed.

This report is published with an additional tool that aims at providing an easy-to-use cause-of-death forecasting framework. The model implemented in the tool relies on the same assumptions as the by-cause model presented in this report. However, the tool also offers the option for a user to input external opinions

about the future pattern of causes of deaths. The authors encourage the reader to familiarize themselves with the cause-of-death framework through this tool.

Section 2: Executive Summary

A first output of this report is an analysis of 11 causes of death that differ from the usual lists for cause-of-death modeling. The purpose of this new classification relies on the analysis of key drivers of mortality improvement or worsening. The decrease of the historical death rates were mostly driven by a decrease in cardiovascular diseases. However, this decrease has slowed in the recent years. The historical rates were also driven by a decrease in deaths due to neoplasm, an increase in deaths due to dementia for old ages, as well as an increase in deaths due to drugs at the young ages.

The authors developed a model based on the classical Lee-Carter framework but extended it to a multivariate setting and adapted it to by-cause modeling using a specific calibration of the future trends. The reason for this choice is that the authors desired to model the full range of ages while capturing the sensitivity of each of these ages to the cause-specific mortality improvements. The resulting forecasts are a decrease in the deaths due to cardiovascular, cerebrovascular diseases, and neoplasm. It should be noted that the speed of decrease is reducing for cardiovascular disease. For the increases in death, dementia is expected to continue to grow, although not as fast as it has been historically. However, dementia will likely still be a major concern for people aged 85 and older. In addition, the model forecasts a fast increase in deaths due to drug abuse at the younger ages.

The authors have compared the model to a standard Lee-Carter model for aggregate mortality. The result is that the by-cause projection is more pessimistic (i.e., leads to higher mortality) for several reasons – 1) the long term forecasts are purely model based, 2) the authors considered in the modeling the most recent trend in the data in the modeling, 3) the projected increase of drug abuse at young ages. These issues are detailed in the report. The authors believe that the by-cause mortality forecast achieves better short-term results than the standard aggregate approach, especially given the two latter features described above. The by-cause mortality forecast enables capturing recent cause-specific trends along with the impact of emerging causes of death. Moreover, the standard model is based on historical data, and the authors believe that an ideal by-cause model should incorporate expert judgement (e.g., health professional opinion) on the future mortality by cause of death. For instance, the forecasts of the author's model for the cause drug abuse is affected by the well-known opioid crisis. If this crisis should end, the forecast of future death rates for the cause of drug abuse would be different. Although the forecasts provided in the report do not account for expert judgement, expert judgement can be input in the dedicated tool that has been designed during this project. This report provides a toolkit for actuaries and other interested parties to model and forecast mortality by cause. The benefits of the work output is threefold:

- First, it relies on a unique redesign of the International Classification of Diseases (ICD) coding, allowing the user of the tool in a more precise analysis of the role of drug and smoking related deaths.
- Second, the modeling framework using the Lee-Carter formulation as a building block is robust and allows the user for analysis of, not only the main parameters for each cause, but also the cross-correlations between the time series underlying the evolution of the cause-specific rates.
- Finally, the report provides a detailed comparison to aggregate forecasts based on a classic Lee-Carter model. This comparison shows that drug abuse increase leads to divergent conclusions for younger ages, but the two types of models tend to agree for higher ages due to rather stable underlying cause-of-death dynamics.

Section 3: Causes of Death Definition and Classification

The purpose of this section is to introduce the general modeling assumptions used for this project. Firstly, the authors introduce the standardized notion of a cause of death. Then, they present the retained classification of causes of deaths, which is a key output of the project. Finally, they explain the calculation of the death rates.

3.1 WHAT IS A CAUSE OF DEATH?

The International Classification of Diseases (ICD) assigns all human deaths to a cause. The ICD is very granular and contains different levels of classification. The different providers of data on death use these ICD classifications to assign a cause to each.

Databases on causes of death are available at granular levels, sometimes with hundreds of causes. The instability of historical data can be a problem at this level of granularity. When forecasting death rates with stochastic mortality, the number of causes of death forecasted must be limited in order to guarantee minimal exposure and therefore, a statistically reliable estimated death rate.

The benefits of using cause-specific death rates are that they provide a good split of aggregate death rates and all of the causes sum up to the aggregate. Note that this is only valid under a modeling assumption discussed in more details in Section 3.4.

3.2 CAUSE OF DEATH CLASSIFICATION FOR THIS PROJECT

The authors used the data furnished by the Human Cause-of-Death Database (HCD) and the exposure from the HMD. The total number of deaths within HCD corresponds to the figures in the HMD. The HCD provides US death counts by gender, age group (every five years), and cause, and for each year between 1999 and 2013.

The available classifications within the HCD are:

- Short list: 16 causes
- Intermediate list: 104 causes
- Full list: relies on a detailed ICD coding, and may vary by country

The HCD was chosen because the method for classifying cause of death is easily comparable to other countries' methods. Furthermore, this dataset provides time series data with causes of death classified according to a constant (fixed) list/classification of causes of death. This is a nice feature of the dataset, since the user does not need to handle the ICD version classification changes over time. However, due to the lag in data processing, calculation, and publication, recent years may not yet be available in the HCD and therefore other data sources may be needed for these missing years, as is the case for this project.

The authors chose to adopt a classification that includes multiple causes from the HCD intermediate list that form the 11 causes of death focused on in this report. This list of 11 causes was designed in collaboration with the members of the Project Oversight Group (POG). Note that the authors had to work with the intermediate list in order to group certain sub-causes. For the purpose of this analysis, the short list granularity was not satisfactory. In the author's opinion, some of the key causes of death to be analyzed from

an actuarial viewpoint were not separable at the short-list level. On the other hand, too granular of a classification makes it difficult to forecast appropriately for all causes of death.

The retained causes list ("working list") is provided in Table 1 and the HCD short list is provided in Table 2. The correspondence between the working list and the intermediate list is detailed in Appendix.

Table 1
WORKING LIST

Cause no	Working list
1	Cardiovascular diseases
2	Cerebrovascular diseases
3	Neoplasms directly induced by smoking (Neosmok)
4	Neoplasms (not directly induced by smoking)
5	Dementia
6	Diabetes
7	Influenza
8	Respiratory diseases
9	Drug abuse
10	External causes
11	Other

Table 2
HCD SHORT LIST

Cause no	HCD short list
1	Certain infectious diseases
2	Neoplasms
3	Diseases of the blood and blood-forming organs
4	Endocrine, nutritional and metabolic diseases
5	Mental and behavioral disorders
6	Diseases of the nervous system and the sense organs
7	Heart diseases
8	Cerebrovascular diseases
9	Other and unspecified disorders of the circulatory system
10	Acute respiratory diseases
11	Other respiratory diseases
12	Diseases of the digestive system
13	Diseases of the skin and subcutaneous tissue, musculoskeletal system and connective tissue
14	Diseases of the genitourinary system and complications of pregnancy, childbirth and puerperium
15	Certain conditions originating in the perinatal period and congenital malformations/anomalies
16	External causes

The following is a comparison between the two lists:

- Cardiovascular diseases (also designated as "Cardiovascular") are grouped in the working list, including most of the short-list causes of heart diseases and "other and unspecified disorders of the circulatory system."
- Cerebrovascular diseases' (also designated as "Cerebrovascular") are the same in both lists.
- Neoplasms are split into "Neoplasms directly induced by smoking" (NeoSmok) and "Neoplasms not directly induced by smoking" in the working list to allow for an analysis of smoking-related neoplasms and to avoid some biased analysis of improvement and increase of neoplasm mortality.

- Dementia in the working list is built from sub-causes of the short-list categories "Mental and behavioral disorders" and "Diseases of the nervous system and the sense organs". The one-to-one correspondence with the intermediate list can be found in the Appendix.
- Diabetes in the working list is built from sub-causes of the short-list categories "Endocrine, nutritional and metabolic diseases," "Heart diseases" and "Diseases of the genitourinary system and complications of pregnancy, childbirth and puerperium". Again, see the one-to-one correspondence with the intermediate list in the Appendix.
- Influenza is built from sub-causes of the short-list category "Acute respiratory diseases."
- Respiratory diseases' (also designated as "Respiratory") are built from sub-causes of the short-list categories "Other respiratory diseases" and "Acute respiratory diseases."
- Drug abuse (also designated as "Drug") in the working list is built from sub-causes of the short-list categories "Mental and behavioral disorders," "External" and "Diseases of the digestive system."
- External causes (also designated as "External") in the working list encompass the remaining sub-causes within the short list "External causes" ; however, this excludes the sub-causes used to build the working list "Drug", as described above.
- "Other" in the working list encompasses all the remaining sub-causes.

The detailed HCD intermediate list of sub-causes used for each of the working list causes is shown in the Appendix.

As discussed above, the HCD data for U.S. mortality ends in 2013. Therefore, to complete the data for 2014–2016, the authors used the data furnished by the Global Burden of Diseases (GBD), which provides the U.S. deaths counts for each gender, by class of age (length five years), by cause (because the classification is not the same as HCD's, a mapping is necessary to achieve the merging), from 1999 to 2016. The correspondence with GBD classification is given in the Appendix, along with the data merging methodology.

3.3 AGE GROUP CLASSIFICATION

By-cause mortality is more volatile than the all-causes mortality due to the limited exposure. This is one reason the data is available for age bands larger than one year. The following age groups are available in the HCD and have been used:

- 0
- 1–4
- 5–9 and each subsequent five year age group up to 90–94
- 95+

Note that for some of the graphics, the age groups will be named according to their HCD prefixes or the first age of the group. For instance, "5" will refer to 5–9.

Although this aggregation by five-year age groups (the standard format provided) creates more stable historical death rates than one year age groups, Gelman & Auerbach (2016) have shown that there might be some aggregation bias within mortality tables. The bias is due to the evolution of the age structure of the inner population within an age group. Since the group is aging over time, it may show a higher or lower number of deaths independent of the underlying (one-year age) mortality rates time pattern. The authors have performed a detailed analysis of possible aggregation biases in the HCD grouping, and have concluded that the aggregation bias was not significant for age group lengths of five years. The results are given in the Appendix.

3.4 DEATH RATE DEFINITION AND INDEPENDENCE ASSUMPTION

For this report, the authors focused on the death rate as the force of the mortality. Thus, the death rate for an age group x, a cause i and a year t is estimated by:

$$\mu_{x,t,i} = \frac{D_{x,t,i}}{E_{x,t}},$$

where $D_{x,t,i}$ refers to the number of deaths by cause i during year t of individuals aged x last birthday. $E_{x,t}$ is an estimate of the so-called exposure-to-risk, that is the total life duration in the year t of individuals aged x last birthday. The exposure does not relate to any cause and the sum of the by-cause estimates gives the total death rate estimate:

$$\mu_{x,t} = \frac{D_{x,t}}{E_{x,t}} = \frac{\sum_i D_{x,t,i}}{E_{x,t}} = \sum_i \mu_{x,t,i}.$$

Beyond this empirical description, below the authors show a theoretical clarification about the definition and main assumption on causes of death in the competing risks framework.

The competing risks framework is based on two causes, *A* and *B*. A cause-specific lifetime is associated with each cause, as

- τ^A : lifetime for cause *A* (such as cancer)
- τ^B : lifetime for cause *B* (such as all other causes)

The random duration τ^A can be interpreted as the lifetime in a world where only cause *A* would exist. The authors denote by τ the total lifetime which can be expressed as the minimum between cause-specific lifetimes as

$$\tau = \min(\tau^A, \tau^B)$$

so that in the competing risks framework life ends when one of the two clocks rings The aggregate death rate (or force of mortality), denoted $\mu(a)$, is defined as the (instantaneous) probability of death before age $a + \delta$ for an individual aged a, for small increment δ. In comparison, the cause-specific death rate $\mu_i(a)$ corresponds to the (instantaneous) probability of death if only cause i exists, given the survival at age a.

The survival function at age a is defined as the probability that all lifetimes by cause will be higher than a.

$$S(a) = P(\tau > a) = P(\tau^A > a, \tau^B > a) = \exp\left(-\int_0^a \mu(y)dy\right)$$

The key issue is that the cause-specific death rate $P(\tau_i < a + \delta | \tau_i \geq a)$ (called "net" probability) cannot be estimated in practice in the general case since one only observes the "duration" of a given cause of death occurs from this cause, while the other durations remain right-censored (it is only known that they are longer than current lifetime). That is, the so-called "crude" probability can be estimated in practice:

$$P(\tau_i < a + \delta | \tau = \tau_i, \tau \geq a)$$

In this work, as it is most often the case in cause-of-death analysis, it is assumed that cause-specific lifetimes τ^A and τ^B are independent, which implies two key consequences:

- The net and the crude death rates are equal. In other words, the (net) cause-specific death rate can directly be estimated from the data using the formula $\mu_{x,t,i} = \frac{D_{x,t,i}}{E_{x,t}}$.
- The survival function can be rewritten as:

$$S(a) = P(\tau^A > a) \times P(\tau^B > a) = \exp\left(-\int_0^a \mu_A(y)dy\right) \times \exp\left(-\int_0^a \mu_B(y)dy\right)$$

Thus, an aggregate mortality rate can be expressed as the sum of the underlying cause-specific rates.

For a more detailed discussion on the dependency structure between cause-specific lifetimes, refer to Dimitrova et al. (2013), Arnold et al. (2018), and references therein.

Section 4: Historical Observations

The purpose of this section is to analyze the historical data obtained with the death rates classification established in Section 3, before any projection. The authors analyze the age structure of the death rates, the distributions of deaths by causes and the historical evolutions of causes of death. Finally, they explain the historical variations of life expectancy as a sum of variations of causes of death.

4.1 AGE STRUCTURE OF THE DEATH RATES

In this section, the authors discuss on the age structure of the mortality rates and focus on the most recent year available: 2016. Note that mortality rates are shown in a logarithmic scale. The all-causes mortality rates are depicted in Figure 1.

Figure 1

ALL-CAUSES MORTALITY IN 2016

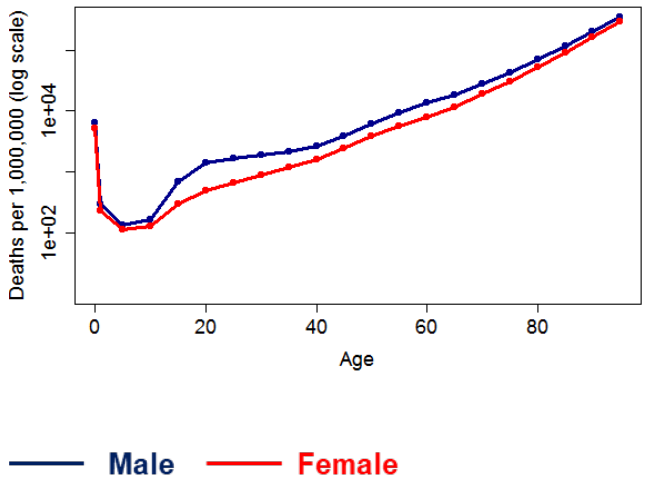

Figure 1 shows a high level of mortality at age 0 due to infant mortality; then the mortality is lowest between one and 15 years. After 15 years, an increase in mortality appears. From 15 to 40, the differences between men and women are quite significant. This section of the mortality curve is referred to as the accident hump, since the additional deaths mainly come from accidental mortality. After 40, the logarithm of the mortality rate seems to be linearly related to age.

Now, let us focus on the repartition by causes of the age structure of mortality at the granularity of the working list as detailed in Section 3. The charts in Figure 2 show the 2016 mortality by cause and age for males and females separately.

Figure 2

BY-CAUSE MORTALITY IN 2016

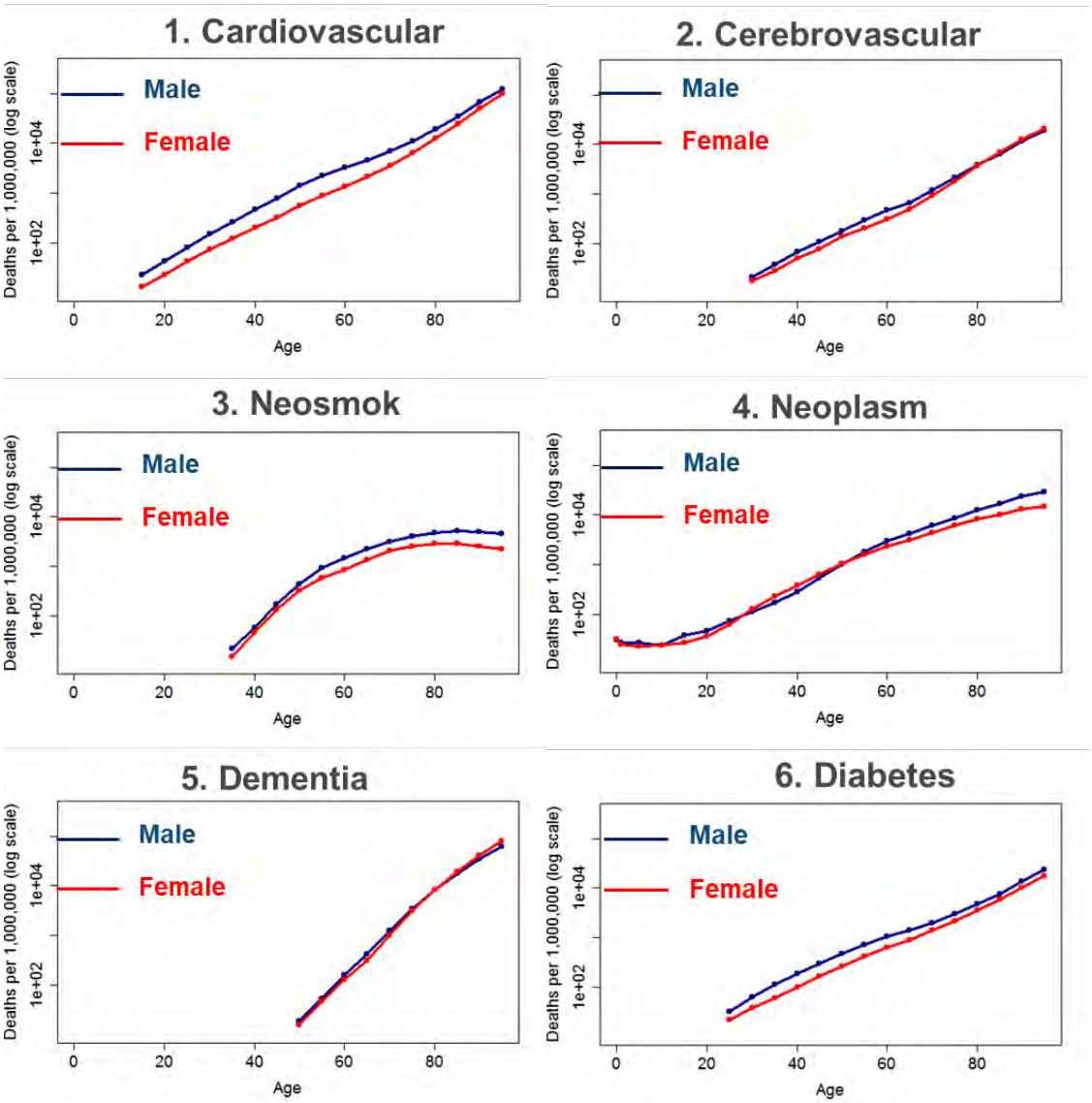

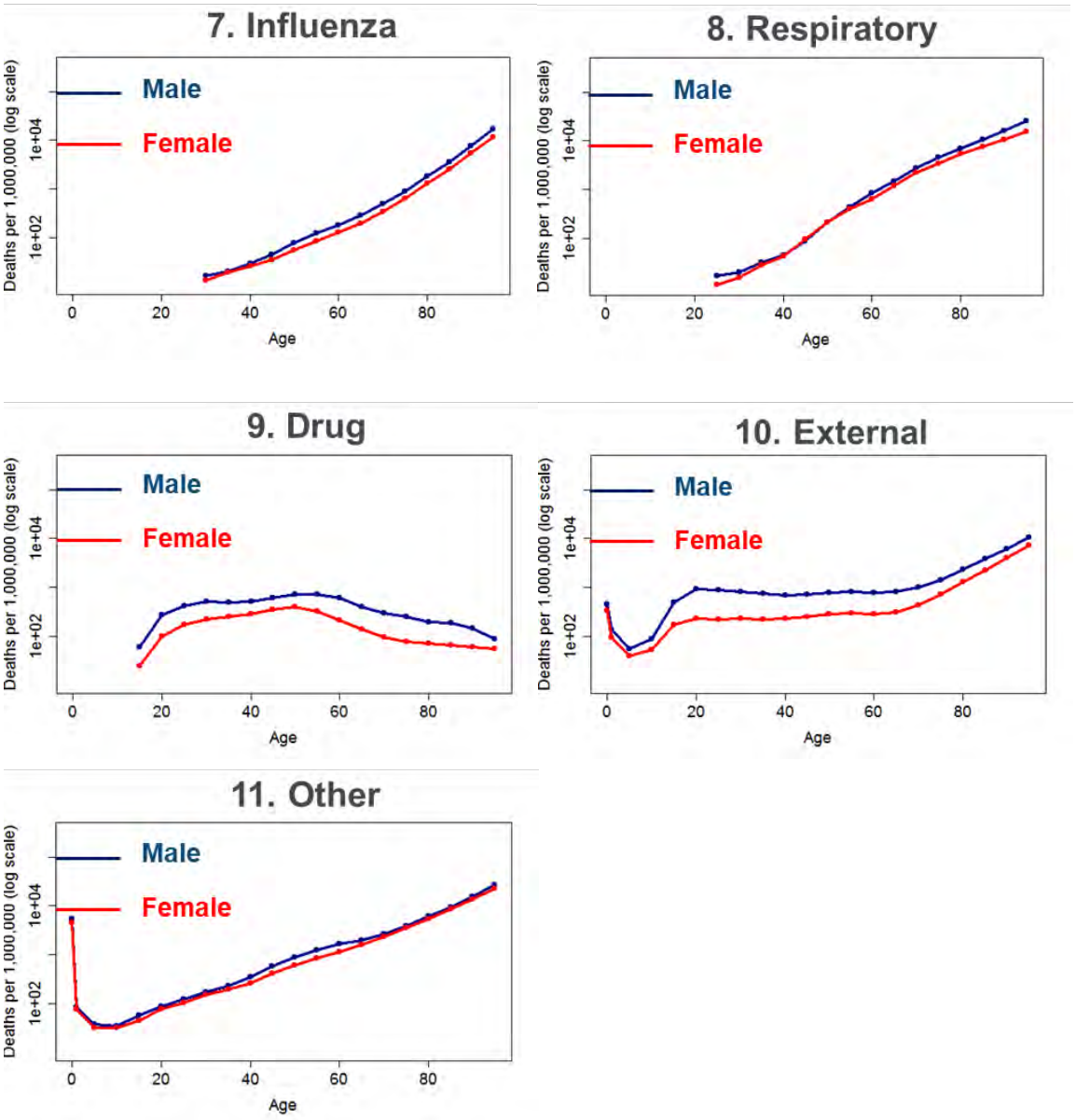

The following are some observations about by-cause mortality shown in Figure 2 above:

- The age structure is different for different causes. For instance, the external cause mortality [10] is constant between ages 20 and 65 and the drug cause mortality [9] is decreasing after age 50, whereas all other causes increase with age.

- Neoplasm [4] and neoSmok [3] mortality is concave by age (on a log scale). Mortality increases quickly up to age 70 and then slows down.

- Dementia mortality [5] has an opposing pattern, exhibiting the fastest increase with age after 70.

- Infant mortality is nearly fully accounted for in the External [10] and Other [11] cause mortality.

- The chart on External cause mortality [10] illustrates the large percentage of accidental mortality between ages 15 and 40 and the gap between male and female mortality due to this cause.

- The male / female gap is also noticeable for drug causes [9] and for cardiovascular diseases [1] before age 75.

- For cerebrovascular [2] and dementia [5], there is almost no gap between male and female mortality.

Figure 3 plots the distribution of deaths by cause for each age group.

Figure 3
DISTRIBUTION OF DEATHS BY CAUSE IN 2016

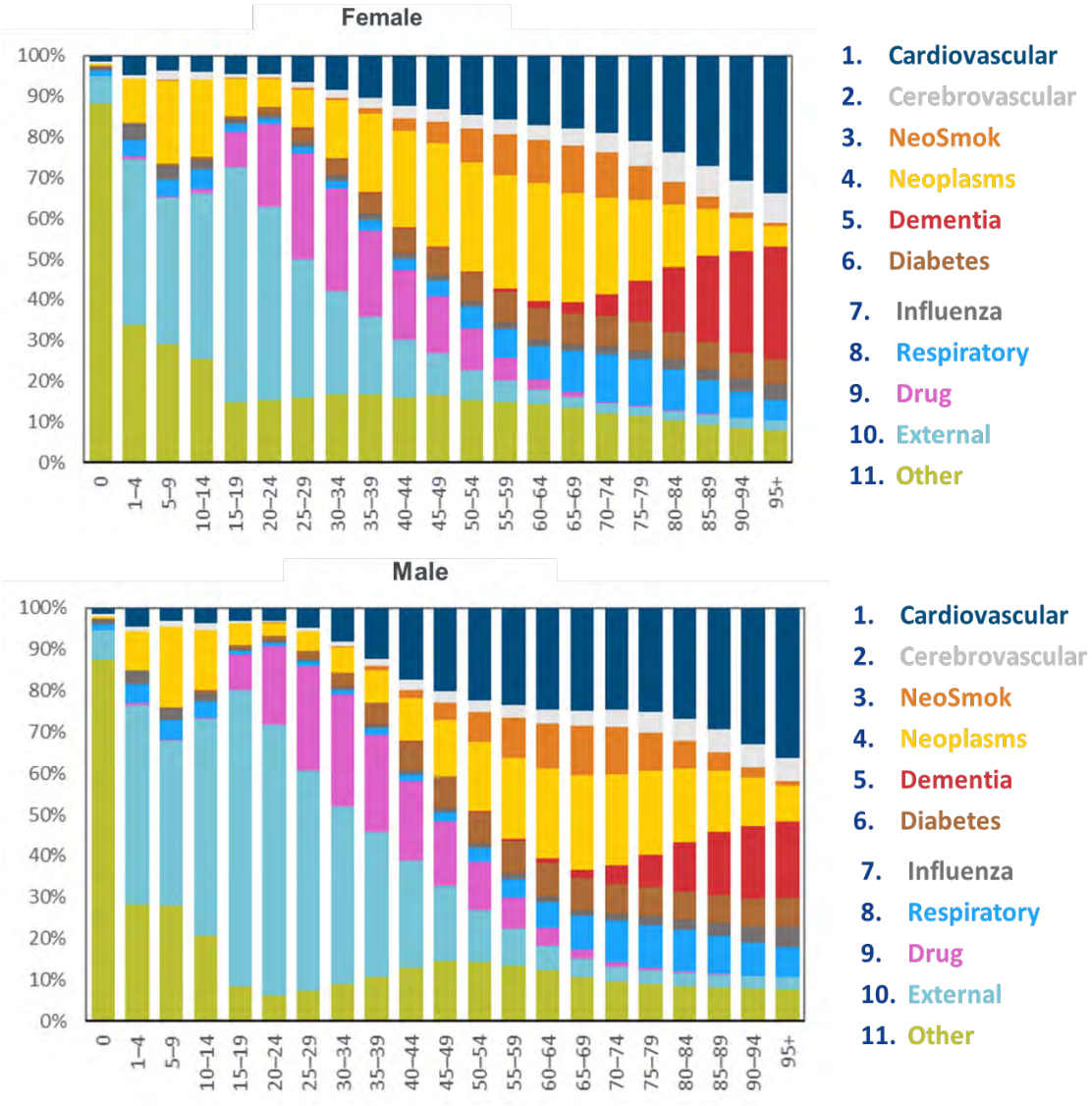

As shown in Figure 3, the main causes of death are for Female:

- Other (i.e., infant mortality), for age group 0.
- External causes and drugs, from age 1 to 35–39.
- Neoplasms with NeoSmok (i.e., neoplasms induced by smoking) and cardiovascular diseases, from 40–44 to 75–79.
- Cardiovascular diseases and dementia, from 80–84 to 95+.

For Male, the main causes of death are:

- Other (i.e., infant mortality), for age group 0.
- External causes and drugs, from age 1 to 45–49.

- Neoplasms with NeoSmok (i.e., neoplasms induced by smoking) and cardiovascular diseases, from 50–54 to 80–84.
- Cardiovascular diseases and dementia, from 85–89 to 95+.

4.2 HISTORICAL EVOLUTION OF THE DEATH RATES

The following charts show the historical evolution of mortality rates. The evolution can vary by age and cause. Similar to the previous section, the authors first focus on an all-causes mortality rates, as shown in Figure 4:

Figure 4
HISTORICAL ALL-CAUSES DEATH RATES

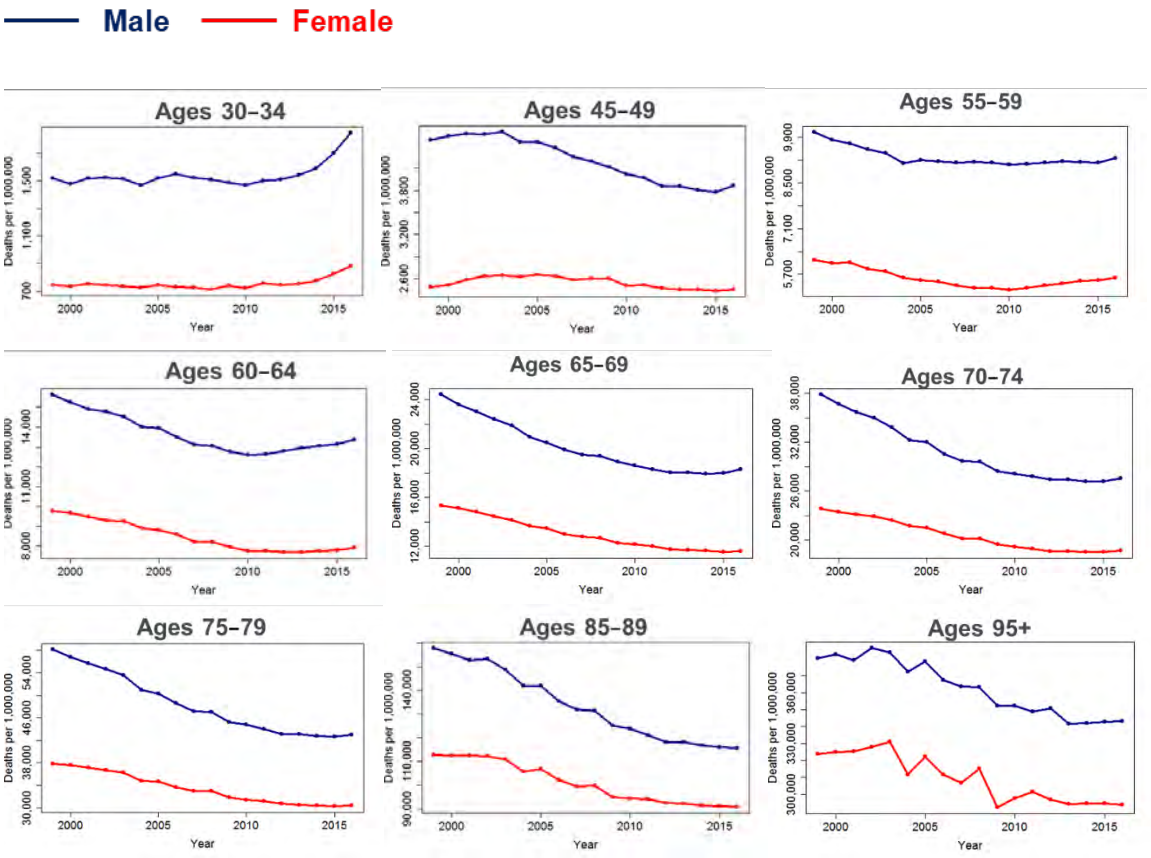

In Figure 4, historical mortality tends to decrease. However, some changes seem to appear after 2010. The most notable is that the direction of mortality improvement has been inversed for some age groups (especially for male age groups 30–34 and 60-64).

The figures 5–8 illustrate the by-cause historical mortality for several age groups. Note that for each age group, the five most important causes of deaths in 2016 are displayed.

Figure 5
HISTORICAL BY-CAUSES DEATH RATES

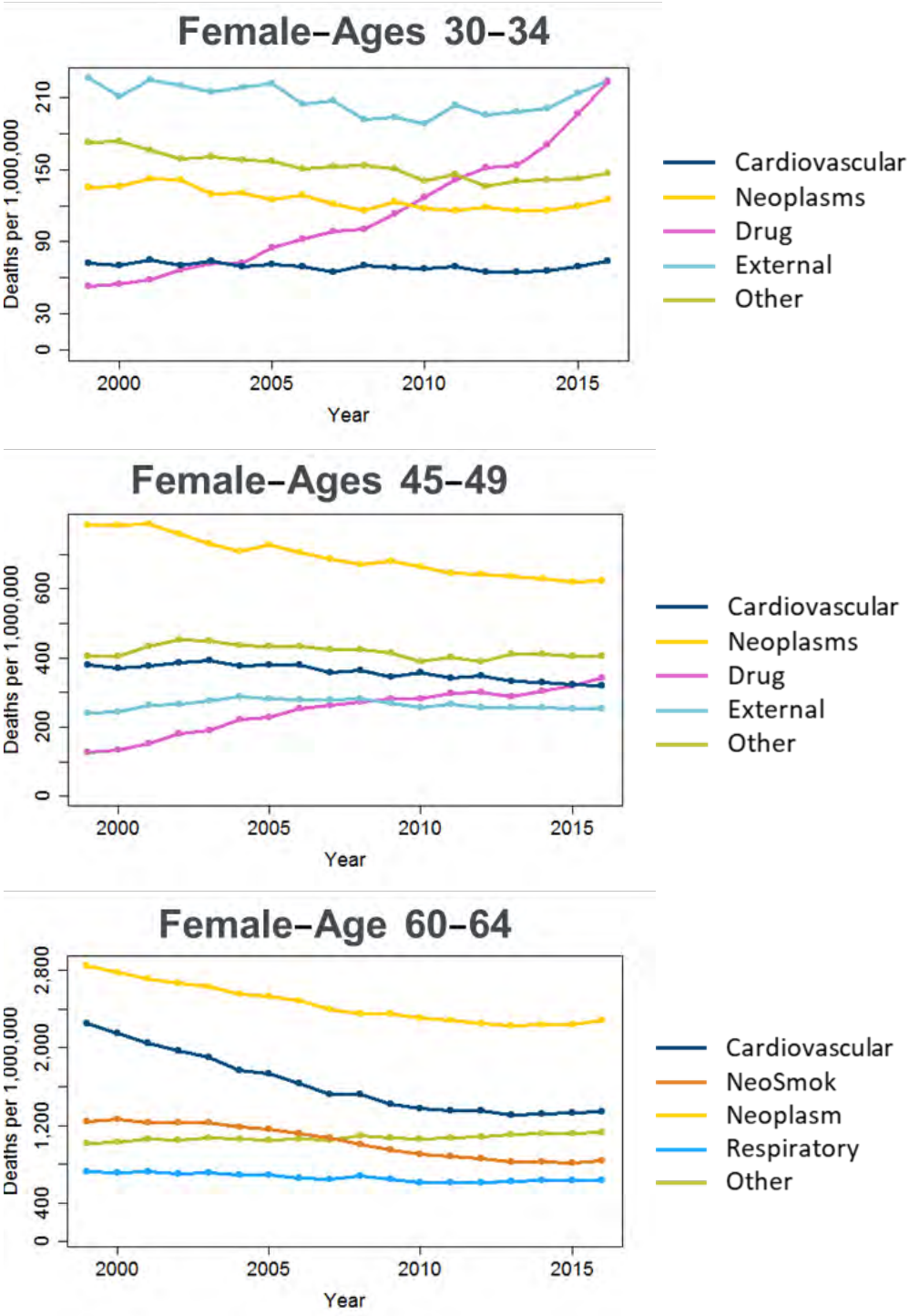

Figure 6

HISTORICAL BY-CAUSES DEATH RATES

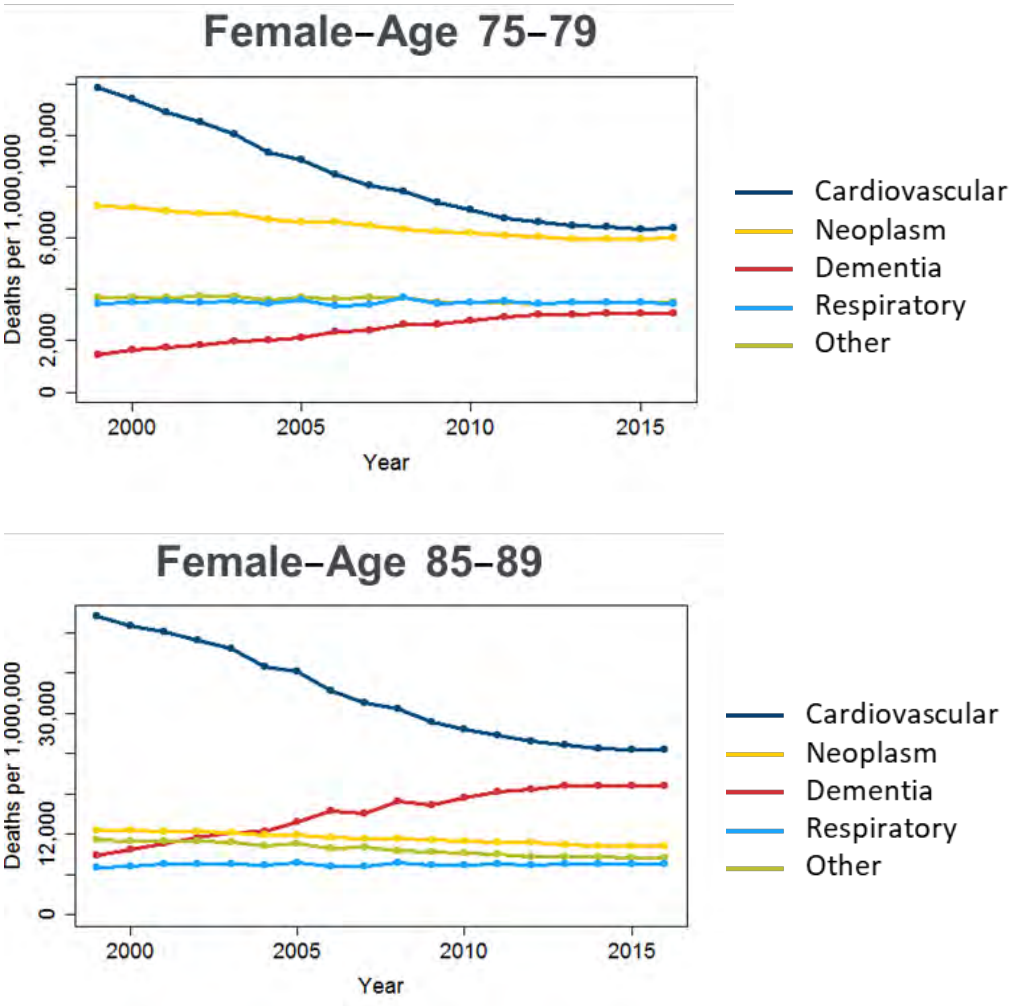

Figure 7

HISTORICAL BY-CAUSES DEATH RATES

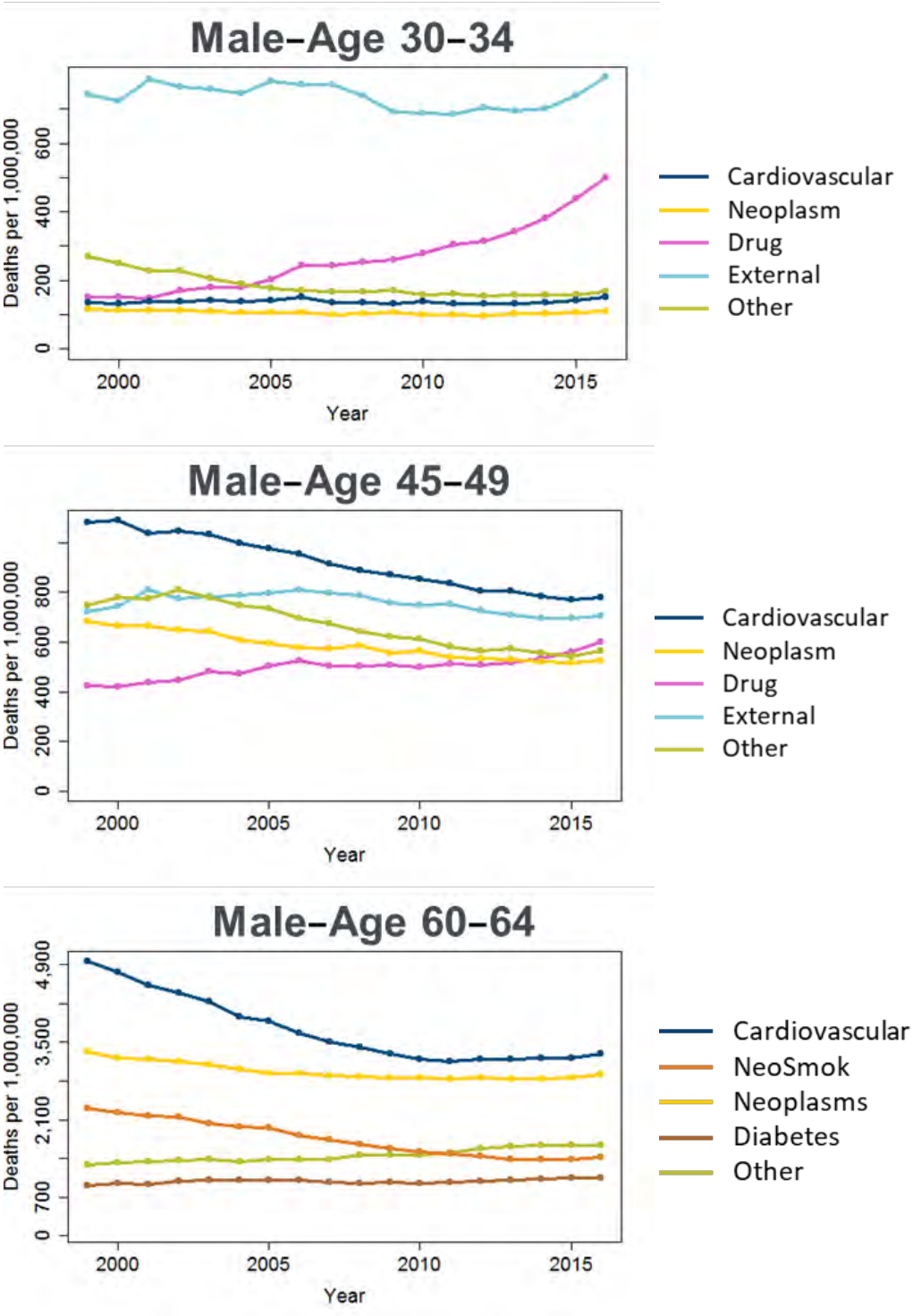

Figure 8
HISTORICAL BY-CAUSES DEATH RATES

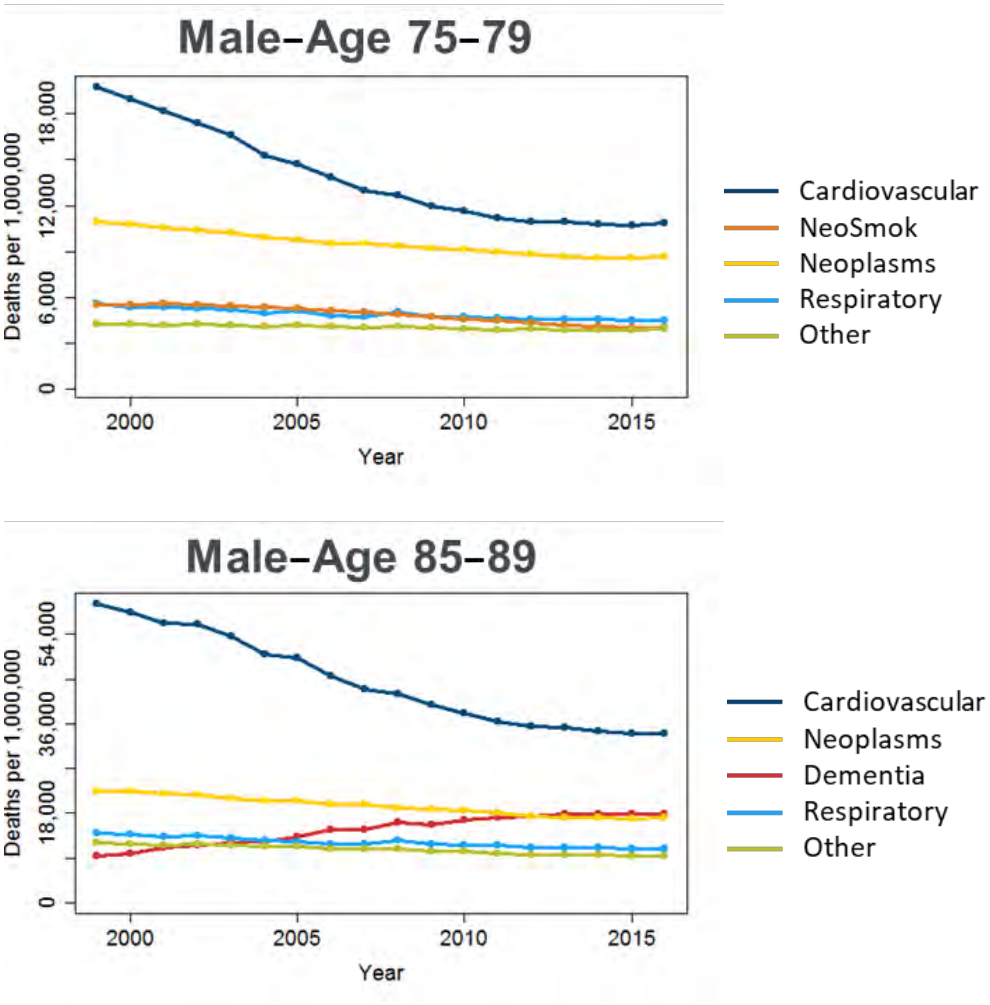

The most notable observations from the above mortality evolution by cause are listed below:

- Cardiovascular death rates have decreased during the 2000s – most notably for females age 60 and older and males age 45 and older. These decreases are one of the key drivers in the decline in aggregate mortality.

- However, after 2009, the trend in declining cardiovascular mortality appears to stagnate. The most radical change is observed for males ages 60 to 64.

- Neoplasms and NeoSmok are the second drivers of the decrease in aggregate mortality. Unlike the cardiovascular trend, this trend appears to continue past 2009 for the most part.

- Drug and Dementia death rates increase over the periods shown in the charts. For Drug mortality, the increase is especially marked for younger ages (30–34). For Dementia, the increase appears to slow starting in 2011.

4.3 HISTORICAL EVOLUTION OF THE LIFE EXPECTANCY

Recall that the period life expectancy is calculated each year t as the expected lifetime for a hypothetical individual experiencing the mortality rates in year t.

Figure 9
HISTORICAL LIFE EXPECTANCY AT BIRTH BY GENDER

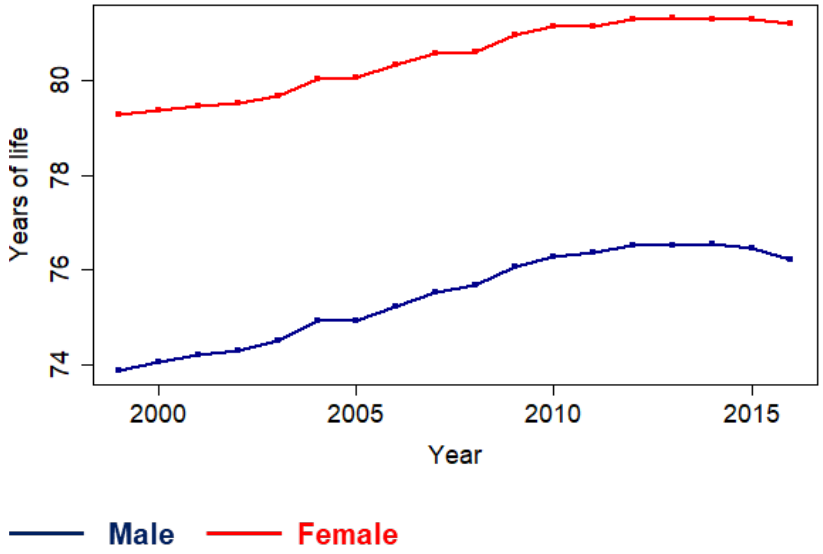

In Figure 9, the historical evolution of life expectancy is characterized by an almost constant increase up to 2010. Thus, male life expectancy evolved from 73.9 years in 1999 to 76.3 years in 2010 (a gain of 2.6 months by year), while female life expectancy evolved from 79.3 years in 1999 to 81.1 years in 2010 (gain of 2 months by year). However, after 2010, the life expectancies are flattening. Thus, in 2016, the life expectancy was 76.2 years for males and 81.2 years for females. In 2016, a decrease of total life expectancy occurs, especially for males. To refine the analysis for high ages, Figure 10 shows the life expectancy at 60 years (defined as the expected remaining period of life for an individual of age 60).

Figure 10

HISTORICAL LIFE EXPECTANCY AT 60 YEARS OLD BY GENDER

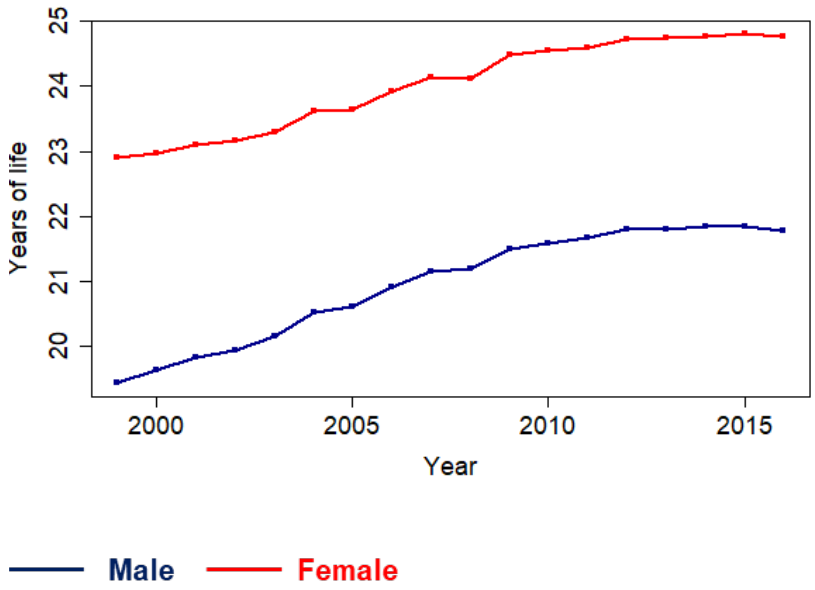

In Figure 10, there is a change of trend over the recent period, but the breakpoint is less clear than for life expectancy at birth. Although drug abuse is the main driver for the decrease in life expectancy at birth after 2008, the death rates for this cause are not material after 60 years old compared to the other causes. Thus, the variations in death rates due to drug causes do not significantly affect the life expectancy at age 60. Rather, dementia plays a role here that creates a flattening (female) or slight decrease (male) in the remaining life expectancy at age 60, even though the dementia death rate increase is slower in the most recent years than in the 2000s.

Using cause-of-death information, life expectancy improvements can be split by the variations due to changes in the risk for each cause, as shown in Figures 11 and 12.

Figure 11

MALE LIFE EXPECTANCY VARIATIONS IN MONTHS INDUCED BY CHANGE IN EACH CAUSE, DURING THE PERIODS

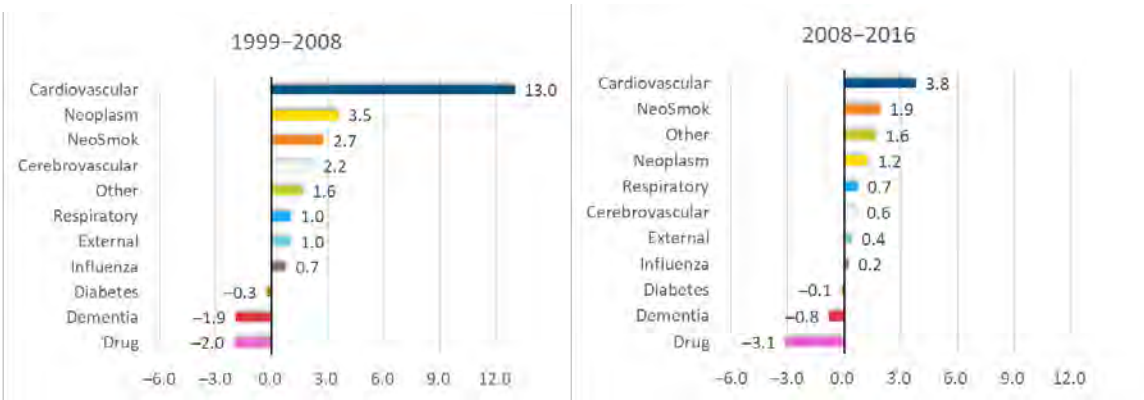

Figure 12

FEMALE LIFE EXPECTANCY VARIATIONS IN MONTHS INDUCED BY CHANGE IN EACH CAUSE, DURING THE PERIODS

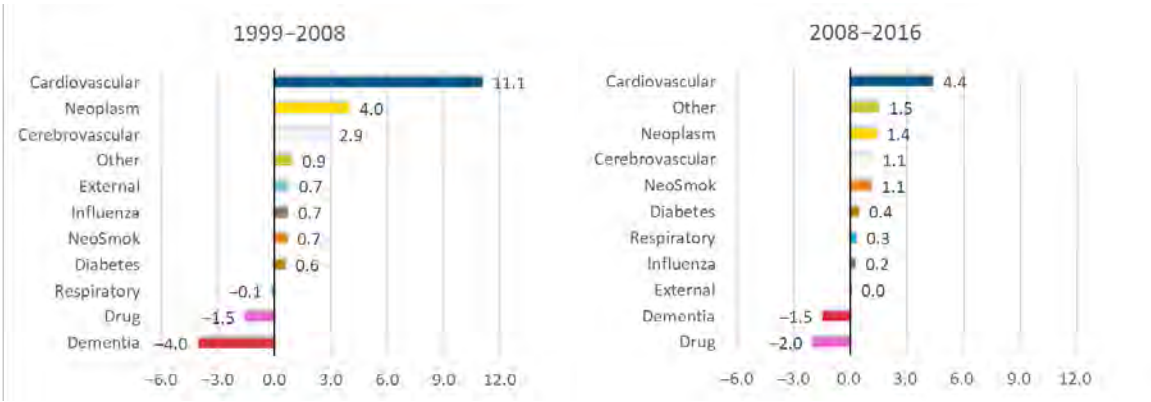

In Figures 11 and 12, there are several insights on the cause-specific impact for life expectancy evolution, that confirm the observations inferred from the by-cause death rates in Figures 5–8. For both males and females, the shortening of life expectancy is mainly due to dementia and drug causes, whereas the lengthening of life expectancy is driven most significantly by the reduction in cardiovascular mortality. More detailed observations on this topic are listed below:

- The share of impact of cardiovascular diseases as a gain reduces after 2008 compared to before 2008.
- Dementia mortality is the main driver for the decrease in life expectancy for females before 2008. After 2008, drug mortality is the main driver for the decrease in life expectancy for both males and females. Variations in the dementia death rates have provoked a four-month decrease in life expectancy during the 1999–2008 period, whereas they have only provoked a 1.5-month decrease in life expectancy during the 2008–2016 period.

Section 5: Cause-of-Death Mortality Modeling

The purpose of this section is to detail the modeling framework developed for the forecasting of cause-specific mortality rates. The authors firstly introduce the usual modeling approaches used for cause of deaths forecasting, and explain the choice of the model (multivariate Lee-Carter model). Then, the authors detail the model calibration, with a specific interest on the trend parameters.

5.1 STATE OF THE ART

Several approaches can be used to forecast mortality rates by cause. The authors chose to examine four main areas found in recent literature, which aim to forecast cause-of-death mortality.

The first approach is to capture the link between causes and a number of clinical factors (such as smoking prevalence, obesity, diabetes, low physical activity) and then stochastically forecast those clinical factors. Such work has been done in, for example, Foreman et al. (2018). However, the authors believe this approach has two limitations:

- It is difficult to apply without the resources of a full team of experts in different medical fields, and
- The modeling framework is too heavy (requires amount of medical/biometric data and a specific model that captures the causal link between such data and the death rates) to be operational in an actuarial context.

A second area of research relies on compositional data analysis. In this framework, an all-cause mortality is forecasted jointly with by-cause proportions of deaths, such that the sum of the proportions over all causes is forced to one. A founding work in this direction is Oeppen (2008), see also, for example, Bergeron-Boucher et al. (2017), Kjærgaard et al. (2018), and Piveteau & Tomas (2018). An alternative approach is also described in Li et al. (2019). That approach to the joint modeling of aggregate and cause-specific mortality helps to provide forecasts of causes in coherence with an aggregate projection. In this project, the authors also focused on challenging an aggregate forecast by some cause-based alternative. Although this is an interesting option, this field is still emerging, and the authors preferred to focus on more proven methods (see the areas below).

The third possible approach is to rely on expert judgment to replicate by-cause target improvements. For instance, large surveys have been conducted by Canudas-Romo et al. (2016). For this project, the authors rely on a modeling viewpoint while still allowing expert judgement to set targets in the model.

Finally, a fourth alternative relies on classical stochastic mortality models, which originate from Lee & Carter (1992), see also Cairns et al. (2009, 2011). Such models have been used to forecast cause-specific mortality in a multivariate form by Alai et al. (2018).

In this project, the authors relied on a multivariate Lee-Carter framework to capture the joint (stochastic) dynamics of the cause-specific death rates, while accounting for a detailed treatment of cause-specific historical breakpoints. The modeling also allows one to input expert judgement in the modeling. Although the results presented in this report do not account for such expert judgement, expert-adjusted forecasts can be produced by using the additional tool.

5.2 LEE-CARTER MODEL

In this project, the authors adapted the Lee-Carter model (1992) to cause of death modeling in a multivariate framework. In this model, the age x time mortality surface of each cause i is decomposed into a static age function $\alpha_{x,i}$ (cause-specific age structure), a time series $\kappa_{t,i}$ driving the cause-specific mortality stochastic

evolution, and an age sensitivity parameter $\beta_{x,i}$ that captures the sensitivity of the age class x to the cause i specific increase or decrease.

In formula, the logarithm of the mortality rate is given as follows:

$$\ln(\mu_{x,t,i}) = \alpha_{x,i} + \beta_{x,i}\kappa_{t,i}$$

The model is calibrated using the likelihood method, assuming that the number of deaths follow a Poisson distribution, see Brouhns et al. (2002).

To project mortality and capture the interaction (correlation) between cause-specific mortality rates, the time series $(\kappa_{t,i})_i$ are jointly modeled and forecasted using ARIMA processes. Typically, a random walk with drift has been shown to provide a reasonable fit, if one properly accounts for historical trend changes, as discussed in next section.

Note that the stochastic mortality modeling within this project has been achieved using the R package StMoMo (Stochastic Mortality Modeling).

As an illustration, the coefficients fitted for the cardiovascular diseases cause of death among the male population are depicted in Figures 13 and 14. $\alpha_{x,i}$ represents the structure in age, which is coherent with the descriptive statistics (see Section Section 4:). $\beta_{x,i}$ allows us to say that mortality improvements benefit the70–85 age groups the most. Note that the variations of $\beta_{x,i}$ before 45 years old are not meaningful because the levels of the cardiovascular death rates are low at these ages. $\kappa_{t,i}$ illustrates that before 2010 gains to life expectancy are fairly constant year after year at most ages, but also that this decelerates after 2010.

Figure 13

CALIBRATED AGE-DEPENDENT PARAMETERS, MALE, CAUSE CARDIOVASCULAR

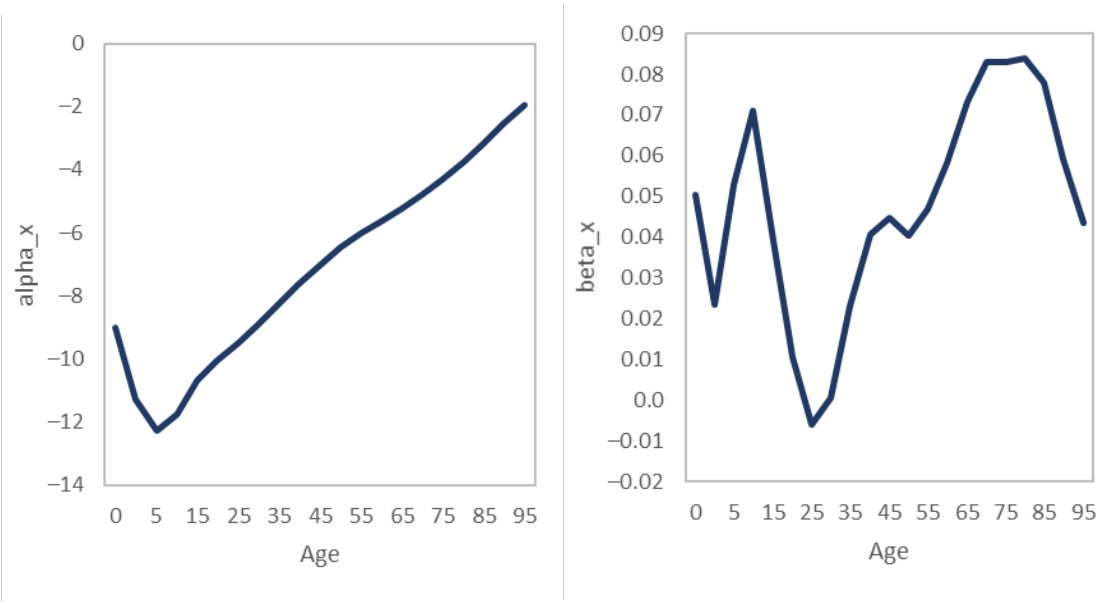

Figure 14
CALIBRATED TIME-DEPENDENT PARAMETERS, MALE, CAUSE CARDIOVASCULAR

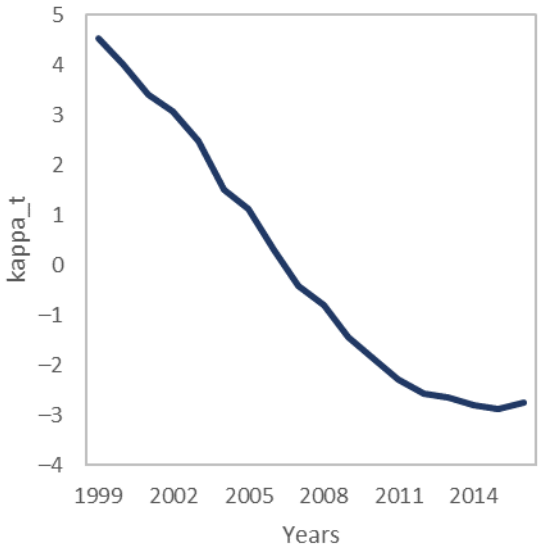

The calibrated values of α, β and κ for both gender and all causes are given in the Appendix.

The methodology of calibration is:

- The authors first calibrated the model separately for each cause of death i, allowing in particular to get the time series parameter $\kappa_{t,i}$.
- For each cause of death, the authors calibrated the $\kappa_{t,i}$ dynamics (ARIMA model) by maximum likelihood estimation.
- To take into account the correlation between the different causes of death, the authors then calibrated a correlation matrix based on the residuals obtained during the calibration of the κ_t dynamics of each cause of death.

5.3 TIME SERIES DYNAMICS

Historically, and in many adaptations of the Lee-Carter model according to the literature, the time component $\kappa_{t,i}$ $1 \leq i \leq m$ is assumed to follow a random walk with drift. This is an ARIMA(0,1,0) process:

$$\kappa_{t,i} = \kappa_{t-1,i} + \Delta_i + \varepsilon_{t,i}$$

with Δ_i , the trend parameter (also called drift), modeling the linear trend of the mortality rates and $\varepsilon_{t,i} \sim N((0, \sigma_i)$, a white noise, modeling the deviation of mortality rates from the trend. By $\Sigma \in \mathbb{R}^{m*m}$, the authors denoted the correlation matrix $\Sigma = cor(\varepsilon_{t,.})$ modeling the dependency between causes.

With this model, $\kappa_{t,i}$ is expected to reflect the mortality trend. This will be decreasing over years when the death rates decrease (cardiovascular, cerebrovascular, NeoSmok, neoplasm, diabetes, influenza, respiratory, external and other) and increasing when the death rates increase (dementia and drug).

The calibration of Δ_i and σ_i can be done with a maximum likelihood estimation from each cause. The correlation coefficients are then determined from the residuals $\varepsilon_{t,i}$.

The random walk with drift assumption may not be satisfied over all the historical periods, and the trend parameters Δ_i can then be calibrated on a more recent historical period for some causes, after validation by breakpoint detection.

5.4 BREAKPOINT DETECTION IN HISTORICAL TRENDS

The forecast of future mortality rates based on a trend calibrated over the entire historical period is not completely desirable because trends are changing. Thus, the authors suggested to first detect the changes in historical trends with a quantitative algorithm. A breakpoint is defined as a historical date at which a statistically significant change in the time series trend is observed. Thus, the trend of the model's time component will only be calibrated over the most recent trend if the algorithm has detected a breakpoint.

The authors used a breakpoint procedure developed by Priyadarshana & Sofronov (2015) based on the Cross-Entropy method. This is a model-based stochastic optimization technique to estimate both the number and the corresponding locations of breakpoints in continuous and discrete measurements. The algorithm is implemented in the R package breakpoint.

The time series used is the time component κ_t of the Lee-Carter model, meaning that there is only one time series per cause. If a breakpoint is detected, both the trend and the volatility of the calibrated model will be changed. The authors only allowed one breakpoint, because the historical period is short. When several breakpoints appear in the graphs, the method chooses to retain the most recent one (see the example of diabetes in Figure 15).

The breakpoint detection method has been statistically and qualitatively validated. For example, the breakpoints retained occur the same year for Male and Female. An adjustment to the breakpoints has been performed for causes diabetes, drug, and influenza because the initial breakpoints were different for Male and Female for these causes.

Figure 15 displays the trends calibrated after breakpoint detection:

Figure 15

HISTORICAL TIME COMPONENT AND RETAINED TRENDS AFTER BREAKPOINT DETECTION

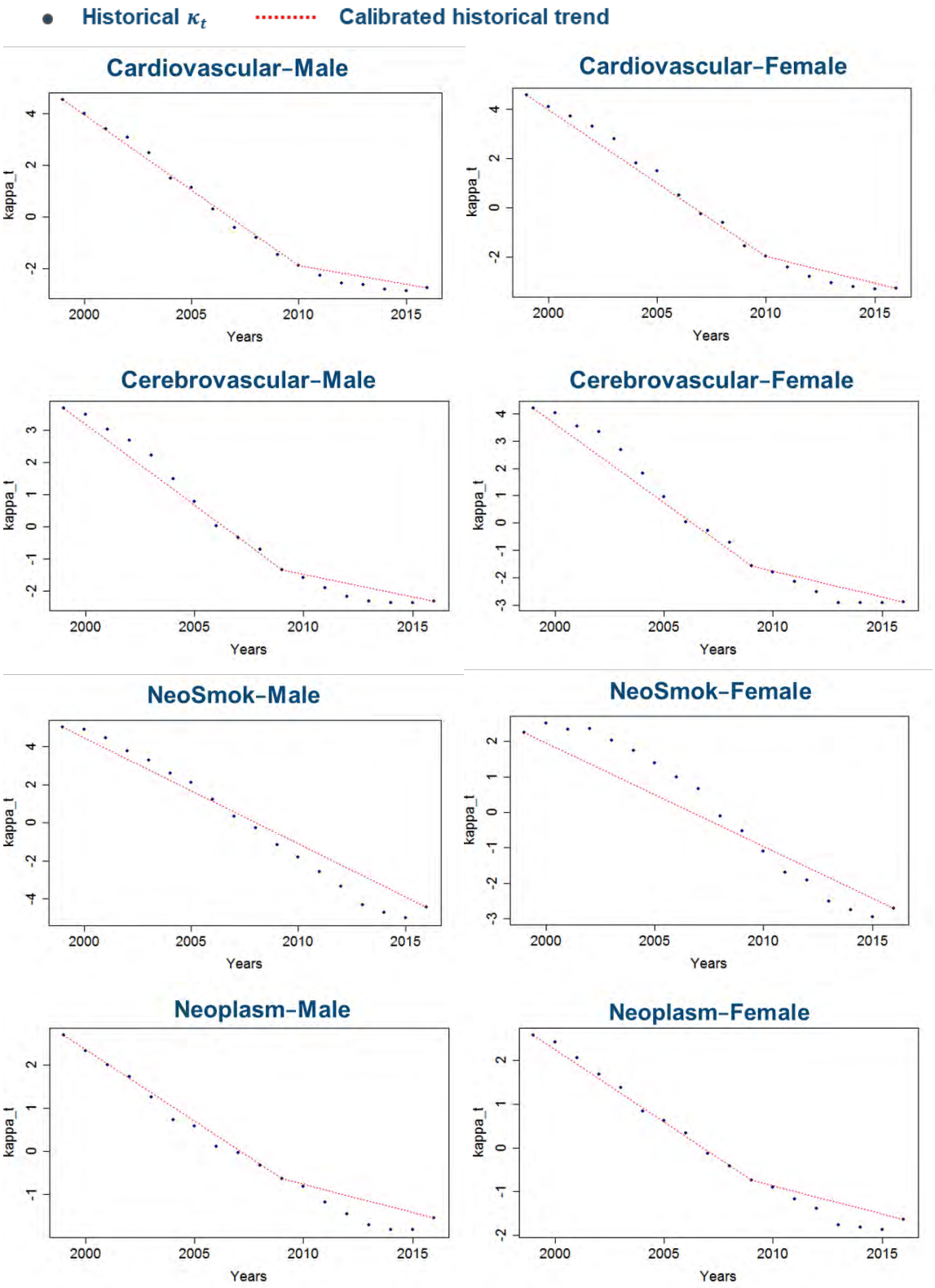

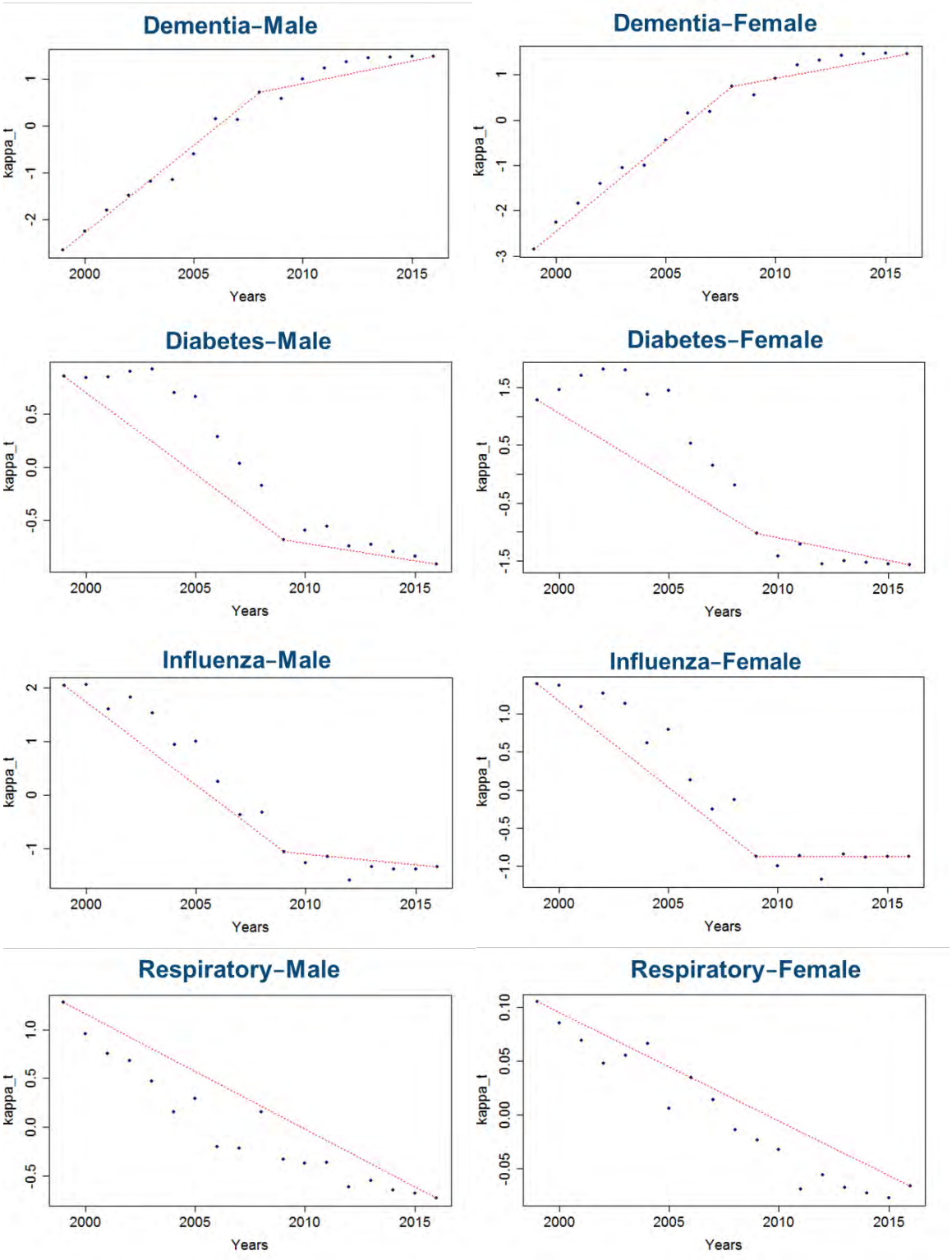

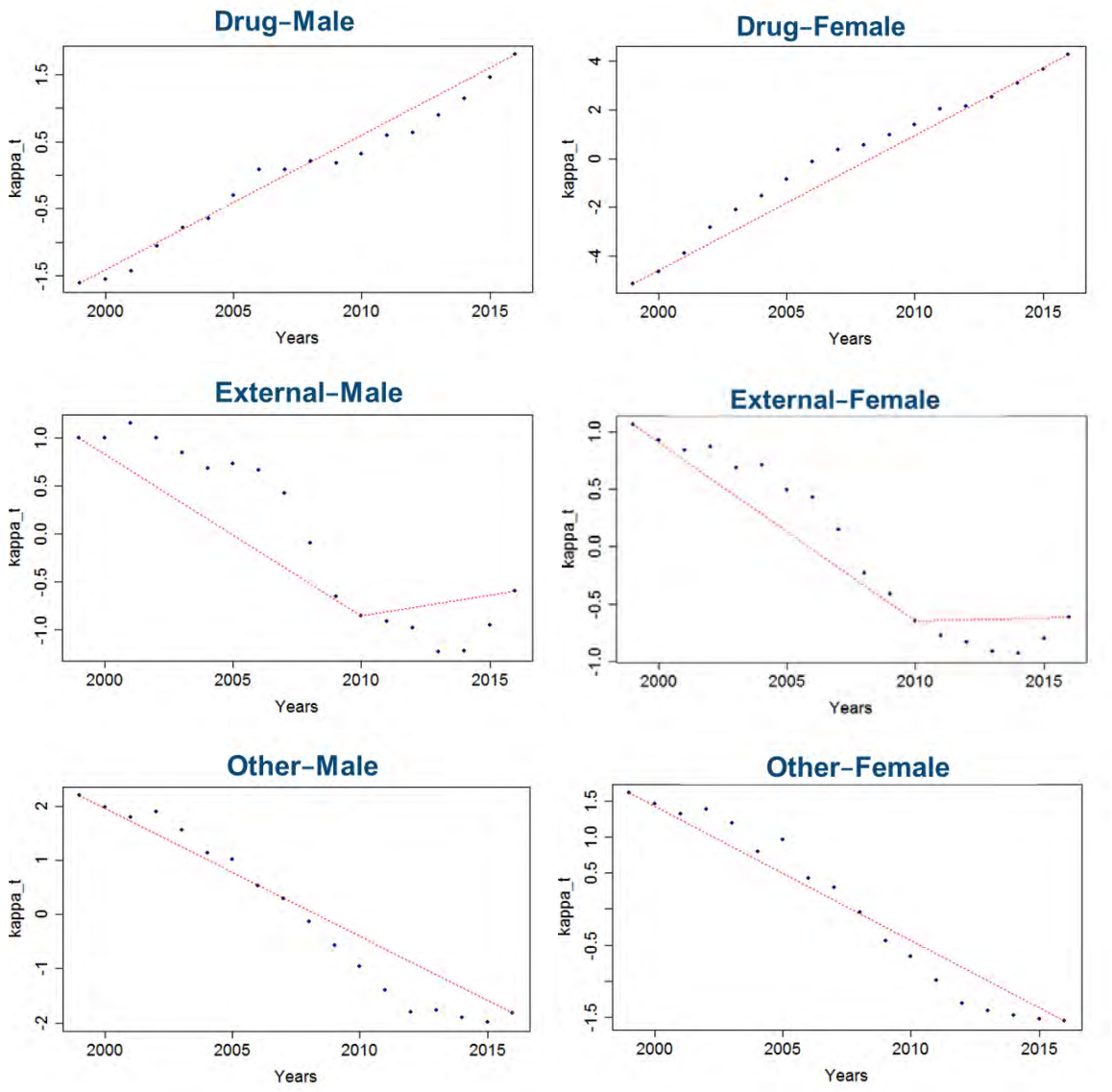

The breakpoint detection method provides interesting results that confirm the observations the authors have made on the recent changes in mortality improvements for some causes.

- For cardiovascular, cerebrovascular, neoplasms, diabetes and influenza causes, a breakpoint is detected, implying a decrease of improvements. The new trends are still decreasing.
- For dementia causes, a breakpoint is detected and the increase in mortality is slower with the new trend than with what it was in the 2000s.
- For external causes, a breakpoint is detected and the new trend is slightly increasing, whereas it was decreasing before.
- For NeoSmok, respiratory and other causes, no breakpoints are detected and the trend is decreasing.
- For drug causes, no breakpoint is detected and the trend is increasing.

The retained breakpoints are listed in the Table 3.

Table 3
BREAKPOINT DATE

Cause of Death	Breakpoint date
Cardiovascular diseases	2010
Cerebrovascular diseases	2009
Neoplasms directly induced by smoking (NeoSmok)	No breakpoint
Neoplasms not directly induced by smoking	2009
Dementia	2008
Diabetes	2009
Influenza	2009
Respiratory diseases	No breakpoint
Drug abuse	No breakpoint
External causes	2010
Other	No breakpoint

An important observation is that the breakpoints are between 2008 and 2010, thus the year 2009 appears to be a key pivot.

The trend parameters are obtained from the most recent trends and the volatility and correlations from the entire period. The calibrated parameters are shown in Tables 4, 5, 6 and 7.

Table 4
CALIBRATED PARAMETERS, FEMALE

Cause of Death	Δ	σ
Cardiovascular diseases	−0.214	0.235
Cerebrovascular diseases	−0.188	0.247
Neoplasms directly induced by smoking (NeoSmok)	−0.292	0.279
Neoplasms not directly induced by smoking	−0.127	0.149
Dementia	0.088	0.193
Diabetes	−0.078	0.336
Influenza	−0.0002	0.289
Respiratory diseases	−0.010	0.021
Drug abuse	0.553	0.221
External causes	0.006	0.123
Other	−0.186	0.184

Table 5
CALIBRATED PARAMETERS, MALE

Cause of Death	Δ	σ
Cardiovascular diseases	−0.143	0.193
Cerebrovascular diseases	−0.137	0.171
Neoplasms directly induced by smoking (NeoSmok)	−0.555	0.372
Neoplasms not directly induced by smoking	−0.129	0.162
Dementia	0.096	0.207
Diabetes	−0.033	0.152
Influenza	−0.040	0.308
Respiratory diseases	−0.118	0.219
Drug abuse	0.201	0.133
External causes	0.043	0.213
Other	−0.235	0.206

There are positive trends for dementia, drug abuse and external causes, whereas the trends are negative for all other causes. These figures are consistent with the historical observations, a negative trend implying a decrease in the death rates. For some causes, it could be different for different age groups due to an inversion

of the sign on $\beta_{x,i}$. The level of the trend and the volatility of the time component are difficult to interpret at this stage because of the variations of $\beta_{x,i}$. The authors show a more detailed development of the trends and volatilities of the death rates by age groups and causes in the Appendix.

Tables 6 and 7 show that the correlation coefficients are globally positive, meaning that an important part of the mortality risk by-cause is explained by a factor common to all causes. Moreover, almost all causes are highly positively correlated with cardiovascular. From a modeling perspective, this captures the fact that time series improvements for cardiovascular mortality provide information that the other causes are likely to experience the same pattern with significant probability. For drug and dementia causes, there are smaller correlation coefficients; this is coherent with the observations, because the historical trend is inversed for these causes as compared to the others. Finally, the limited number of observations may explain instabilities in the correlation matrix, especially when looking at the correlation coefficients between two small causes. For instance, a high negative correlation is observed between respiratory and influenza (−66%) for female, whereas it is positive for male (64%). Keep in mind that the correlation matrix is not involved in the central trajectory forecasts but only to derive confidence intervals.

Table 6

CORRELATION MATRIX, FEMALE

	Cardio.	Cerebro.	NeoSmok	Neoplasm	Dementia	Diabetes	Influenza	Resp.	Drug	External	Other
Cardio.	100%	61%	28%	52%	39%	65%	71%	−43%	12%	−4%	75%
Cerebro.	61%	100%	55%	40%	4%	50%	42%	−17%	17%	14%	50%
NeoSmok	28%	55%	100%	57%	−17%	37%	1%	22%	36%	70%	42%
Neoplasm	52%	40%	57%	100%	19%	13%	10%	6%	15%	28%	30%
Dementia	39%	4%	−17%	19%	100%	23%	44%	−27%	5%	−28%	3%
Diabetes	65%	50%	37%	13%	23%	100%	77%	−53%	41%	7%	68%
Influenza	71%	42%	1%	10%	44%	77%	100%	−66%	22%	−19%	65%
Resp.	−43%	−17%	22%	6%	−27%	−53%	-66%	100%	−10%	47%	−50%
Drug	12%	17%	36%	15%	5%	41%	22%	−10%	100%	58%	35%
External	−4%	14%	70%	28%	−28%	7%	−19%	47%	58%	100%	16%
Other	75%	50%	42%	30%	3%	68%	65%	-50%	35%	16%	100%

Table 7
CORRELATION MATRIX, MALE

	Cardio.	Cerebro.	NeoSmok	Neoplasm	Dementia	Diabetes	Influenza	Resp.	Drug	External	Other
Cardio.	100%	60%	48%	65%	23%	44%	66%	54%	27%	17%	66%
Cerebro.	60%	100%	56%	52%	−23%	38%	52%	31%	−5%	21%	60%
NeoSmok	48%	56%	100%	63%	−6%	25%	28%	9%	24%	66%	54%
Neoplasm	65%	52%	63%	100%	−21%	−1%	22%	32%	14%	39%	64%
Dementia	23%	−23%	−6%	−21%	100%	20%	17%	16%	34%	12%	−24%
Diabetes	44%	38%	25%	−1%	20%	100%	69%	41%	34%	43%	43%
Influenza	66%	52%	28%	22%	17%	69%	100%	64%	43%	9%	58%
Resp.	54%	31%	9%	32%	16%	41%	64%	100%	18%	−13%	34%
Drug	27%	−5%	24%	14%	34%	34%	43%	18%	100%	45%	45%
External	17%	21%	66%	39%	12%	43%	9%	−13%	45%	100%	41%
Other	66%	60%	54%	64%	-24%	43%	58%	34%	45%	41%	100%

5.5 INCLUDING EXPERT JUDGEMENT

Including some targets based on expert judgement could be done with an extension of the Lee-Carter model. From a modeling perspective (the model definition is given in the following section), one can only change the trend parameter Δ in the time component forecast $\kappa_{t+1} = \kappa_t + \Delta + \sigma\varepsilon_t$ to reach, for a central trajectory, the target. The other parameters remain unchanged. The target would be the yearly improvement rates for some age groups (or for an age-aggregated death rate) to be used over a forecasting period.

The target for cardiovascular diseases or neoplasms could be obtained from the reports of some specialized organizations (such as American Heart Association and American Association for Cancer Research). It seems the experts believe that improvements for cardiovascular risk will be lower in the near future than what past experience shows. However, improvements for cancer risk may stay at an equivalent level.

The choice of the quantitative targets and the selection of targets for the other causes need to be determined.

A possible choice of modeling is to use expert judgment targets for some causes and forecast the others with available historical data. The choice of targets and of causes to which expert judgment should be applied is key, and depends on the view one has about future mortality risk. Thus, in the base model shown in this report, no expert judgment target is applied. However, the authors encourage readers to use their own targets if they believe this to be a better approach for some causes, than using a full model driven by historical forecasting. These adjustments can be performed through the tool available with this report.

Section 6: Cause-of-Death Mortality Forecasting

This section displays the mortality forecasts resulting from the developed model. The authors then compare the results of their model to the mortality projections of a classical model based on aggregated mortality. For the models used in this report, the trajectories are forecasted 15 years ahead. Since the models have been calibrated over 18 years of historical data, a reasonable limit for realistic projections may be 2030.

6.1 DEATH RATES BY CAUSE OF DEATH

This report displays the result of the projection for the Lee Carter model, where the κ_t follows a random walk with drift. The calibration period of the model is between 1999 and 2016. The projection horizon is 2031 (15 years of projection). The fan charts plotted (see Figures 16–xx) represent level 2.5%, 10%, 25%, 75%, 90% and 97.5% percentiles.

The by-cause historical mortality is displayed for several age groups. For each age group, the five most important causes of death in 2016 are shown.

Figure 16
PROJECTED BY-CAUSE DEATHS RATES

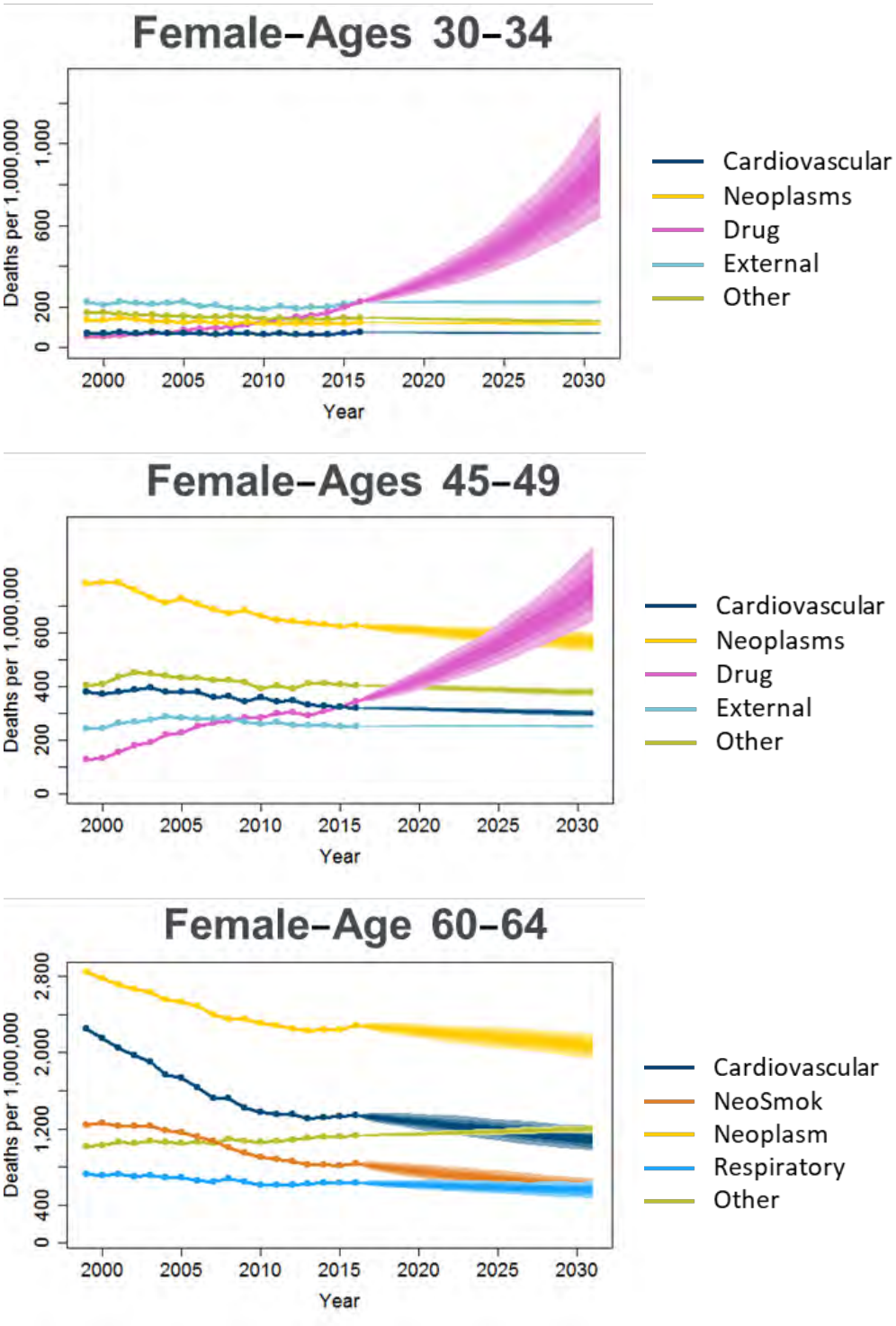

Figure 17
PROJECTED BY-CAUSE DEATHS RATES

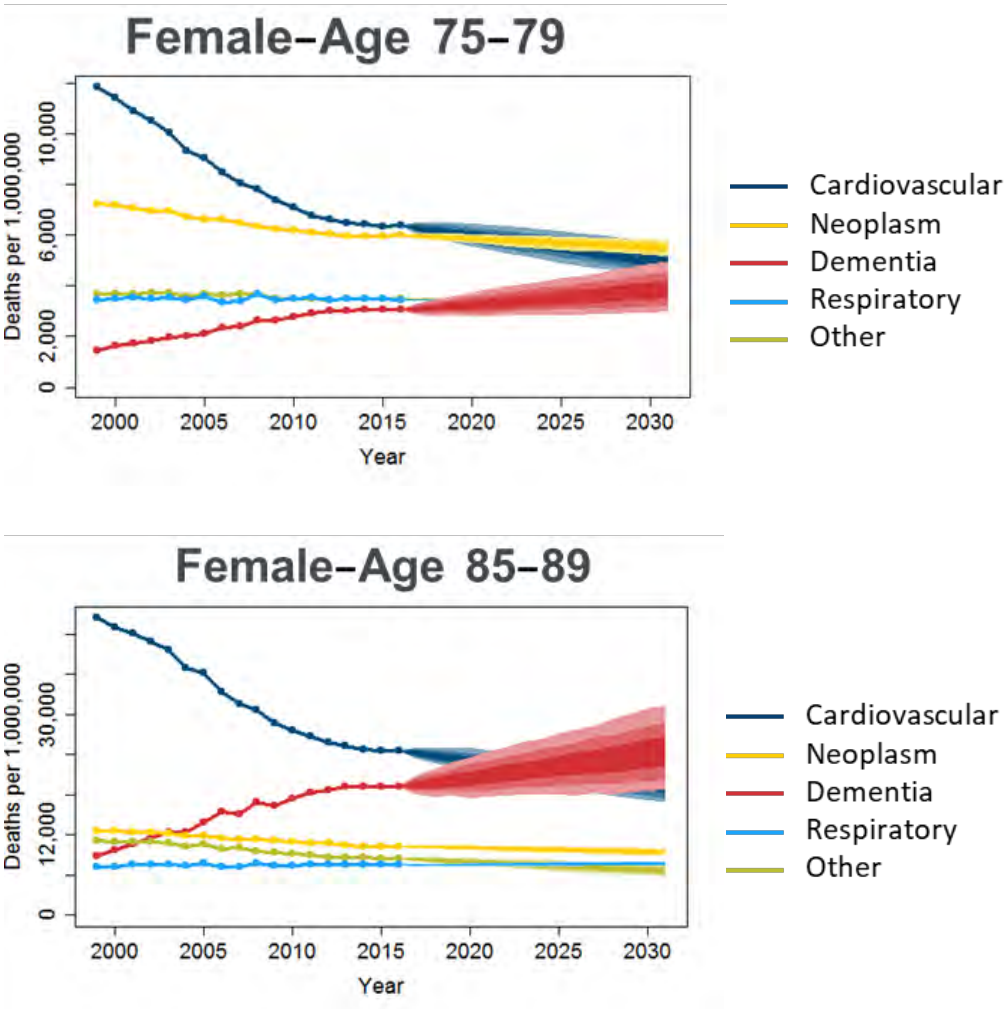

Figure 18
PROJECTED BY-CAUSE DEATHS RATES

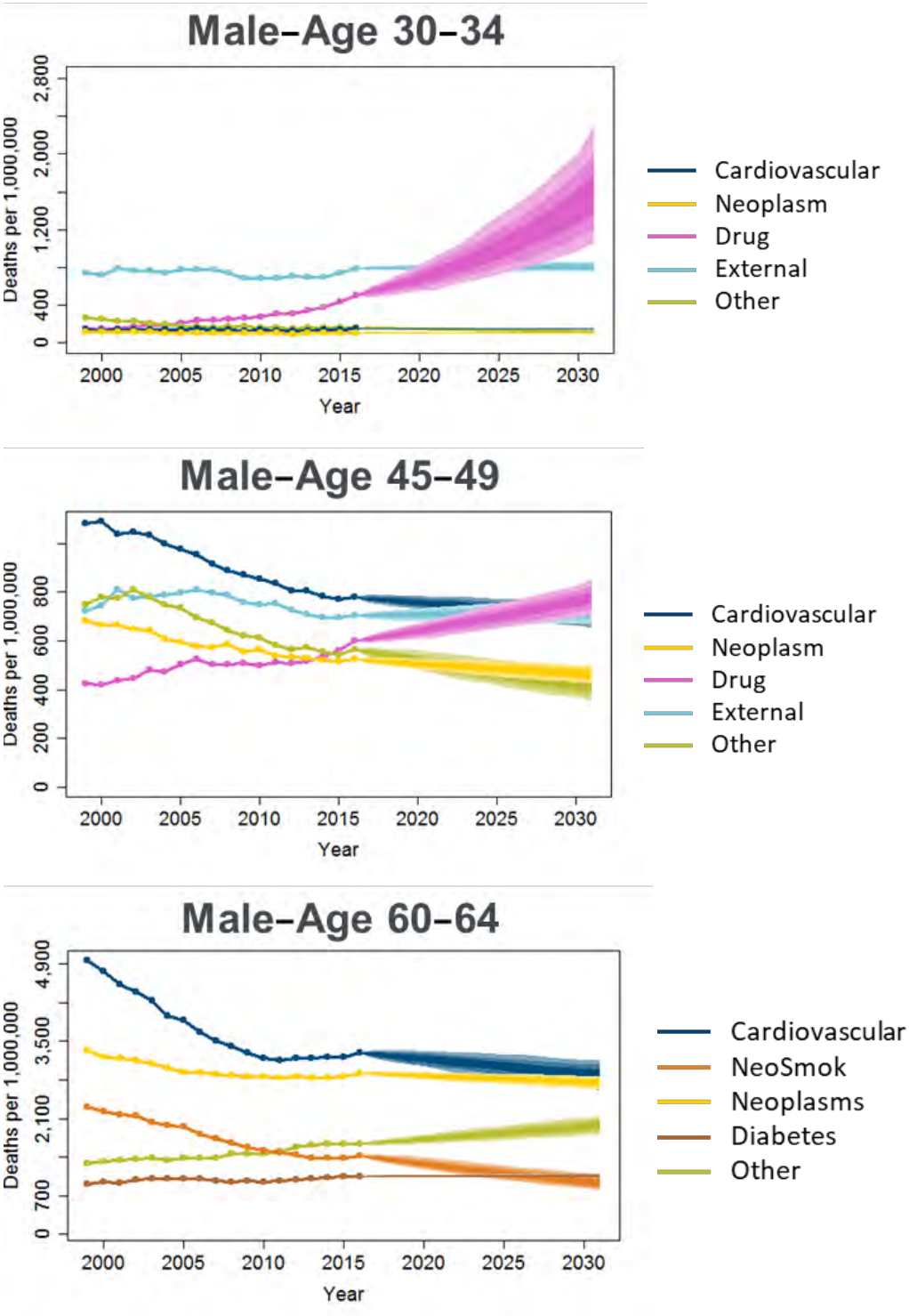

Figure 19
PROJECTED BY-CAUSE DEATHS RATES

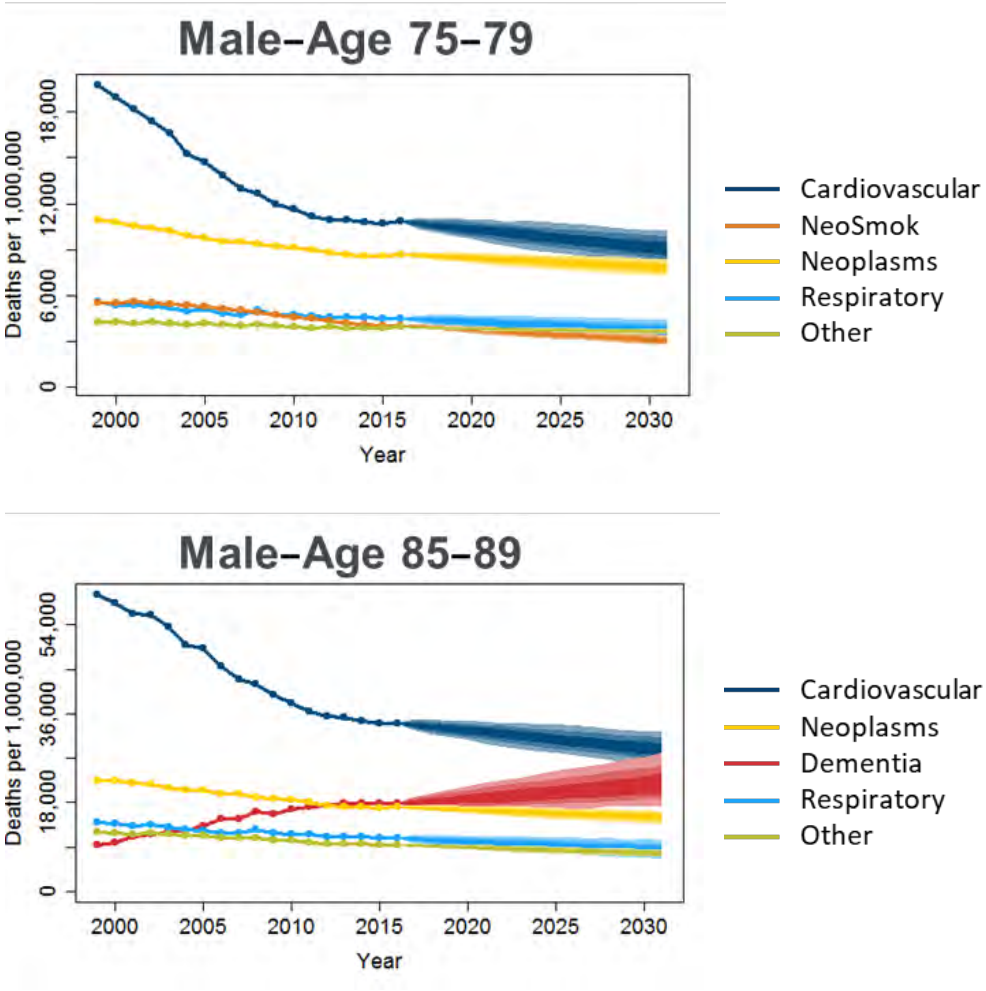

Due to the exponential increase of the mortality rates for drug causes during the historical period, the model forecasts a huge increase in this cause of death for younger ages. This is especially visible for young women in age group 30–34 where drug causes are forecasted to be the highest cause of death in 2017. However, for males, the external causes will remain the highest cause until 2020–2026 for the same age group.

For older ages, the increase in dementia causes is significant. This cause of death is forecasted to become the highest for females ages 85–89 between 2025 and 2030. For males, cardiovascular risk would still remain the most significant cause in the near future.

The model projects a decrease in death rates for cardiovascular diseases. However, breakpoint detection is important in the modeling when observing the cardiovascular forecast for ages 60–64 for males. It would not have been reasonable to extend the fast decrease observed during the 2000s into the future.

For neoplasms, a decrease in death rates is observed. For most age groups, the speed of decrease is comparable to what is forecasted for cardiovascular. However, for neoplasms induced by smoking (NeoSmok), the speed of decrease is even more significant, for males age 60–64. This cause was outpaced by other causes in 2010 and may be outpaced by diabetes causes by 2030. Nevertheless, the model relies on

the assumption that NeoSmok will continue to decrease as fast as it did in the past, which may not materialize in a mid-term future. In a situation where the smokers sub-population would become negligible, this would imply that no aggregate mortality gains would be induced by a decrease in smoking-related neoplasms.

For external causes, forecasted death rates are nearly constant over time and have a low level of volatility. In some other studies about cause of death, external causes may be merged with drug causes, leading to very different conclusions on this subject.

For other causes, we observe an increase for age group 60–64 for both genders. All other groups show level or decreasing mortality rates for this cause. The other causes group contains very different sub-causes; infections, neurological disorders, some mental diseases, skin diseases to name a few, thus it is difficult to speculate on the reasons for the different pattern in the one age group.

For cerebrovascular, diabetes, influenza and respiratory causes, the death rates are low today and are forecasted to remain at low levels for all age groups.

6.2 DEATH RATES AND LIFE EXPECTANCY WITH THE BY-CAUSE MODEL

The figures at a cause level are informative; however, it is also important to analyze the aggregate level of death rates (defined as the sum of by-cause death rates) produced by the model. Figure 20 plots the death rates forecasted for different age groups by gender:

Figure 20

PROJECTED MORTALITY RATES WITH THE CAUSE-BASED MODEL (LEFT: FEMALE, RIGHT: MALE)

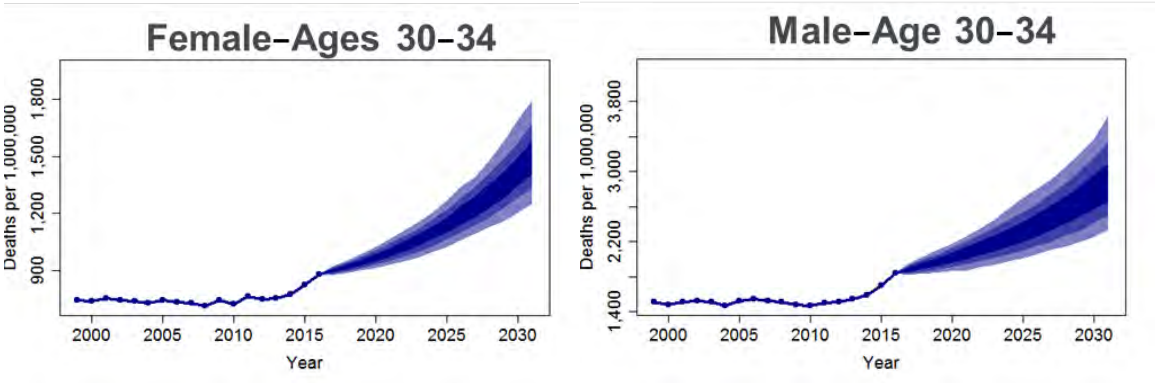

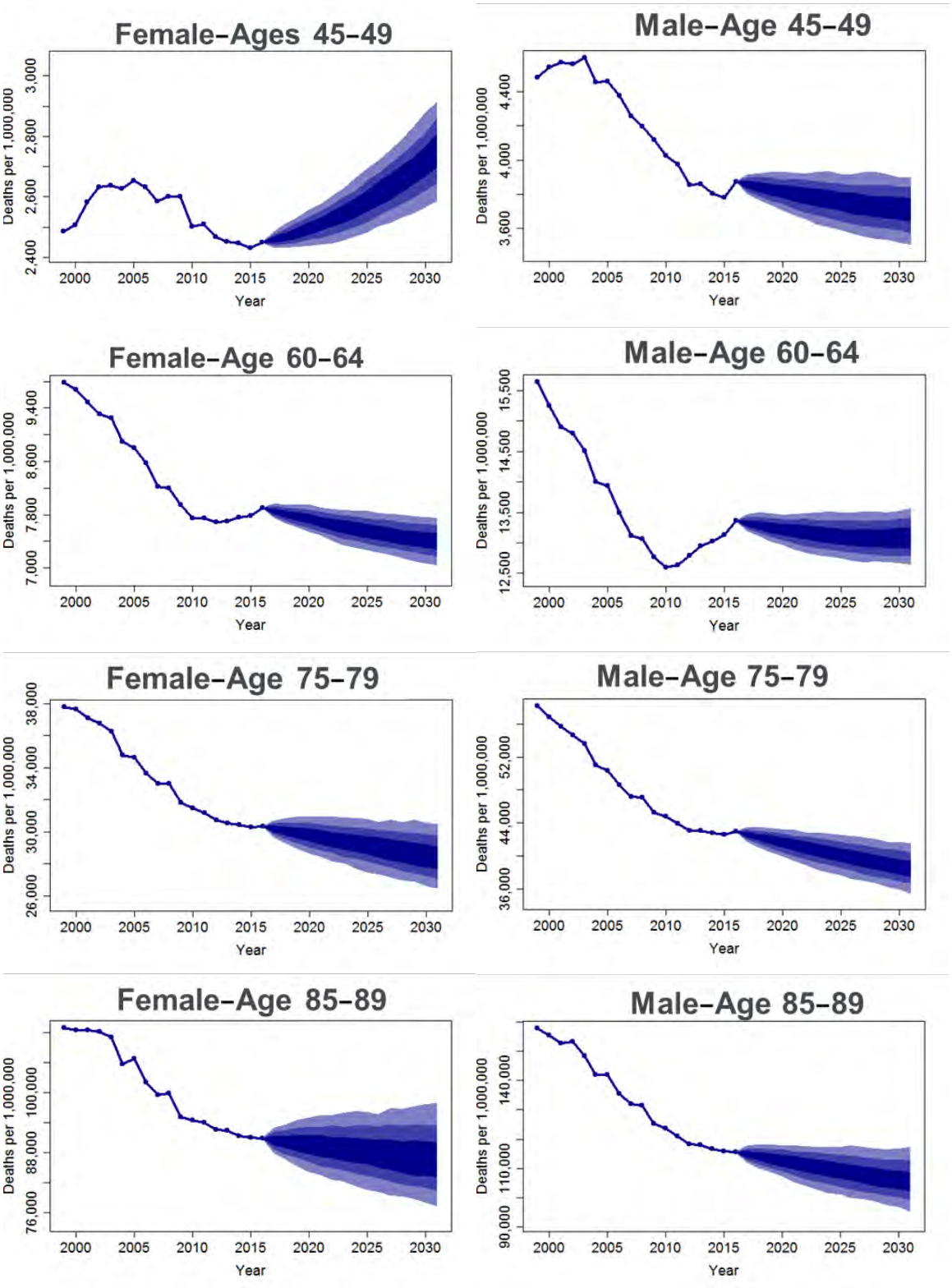

For some age groups, the mortality is not following a linear trend. This is reasonable, because the by-cause modeling framework aims at explaining trends at the cause level and not at an aggregate level.

For younger ages, the mortality is expected to increase at some point because the increase in drug causes is projected to be stronger than the decrease in all other causes. The gap between women and men in terms of death rates is forecasted to reduce over time. The model is more pessimistic for women.

For females ages 60 and higher and males ages 45 and higher, the death rates continue to decrease in the future at a relatively slow pace. We observe a higher volatility for females, mainly due to the dementia volatility.

6.3 COMPARISON BETWEEN A BY-CAUSE MODEL AND AN ALL-CAUSES MODEL

The objective of this section is to compare the results of the by-cause model with a classical Lee-Carter model on aggregate mortality, the "all-causes model." For consistency purposes, the authors have restricted the calibration period of the all-causes model to the period used for the by-cause model. Moreover, no breakpoint detection is used in the all-causes model. Finally, for this section, the authors do not display the confidence interval but only the central trajectories of the forecasts.

Figure 21 compares the death rates for age groups 40–44, 65–69 and 85–89.

Figure 21

PROJECTED DEATH RATES WITH THE BY-CAUSE AND ALL-CAUSE MODELS (LEFT: FEMALE, RIGHT: MALE)

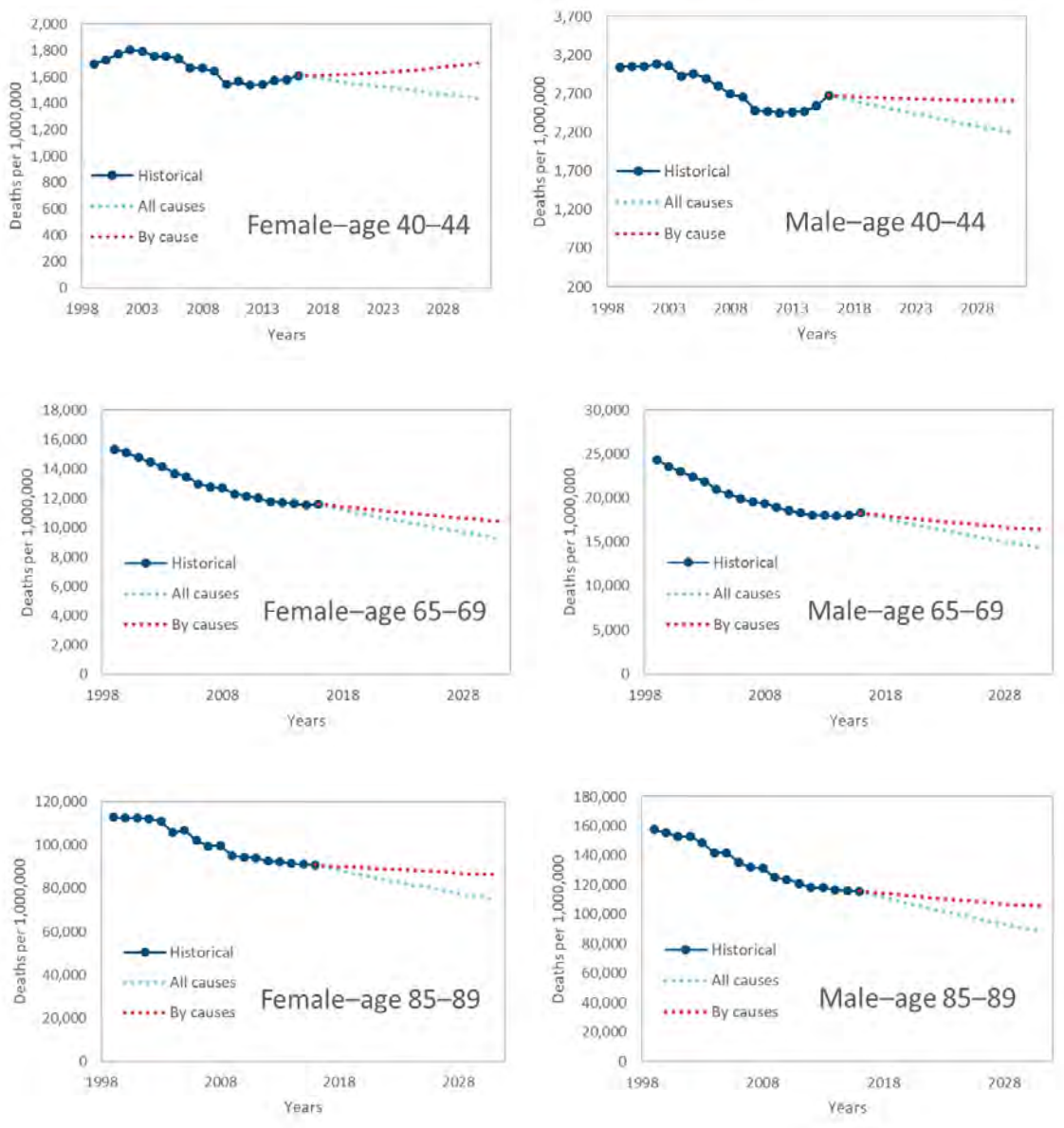

The by-cause projection is more pessimistic than the all-causes projection for both gender and all age groups. This phenomenon has been mentioned by Wilmoth (1994). The pessimism of the by-cause projection is due to the increased importance with the time of projection of the cause of death with the more adverse historical trend, for instance, drug at intermediate ages for females.

For the age group 65–69, the deviation between the two models is smaller. The drug and dementia causes are not material for this age group, thus the trends of the main causes (cardiovascular, neoplasm and NeoSmok) are similar to the all-causes model trend.

Note that the pessimism of the by-cause model is to be nuanced by the fact that no breakpoint detection has been used for the all-causes forecasts. Section 7 of the Appendix contains the same comparison using

breakpoint detection for the all-causes model. In that case, the by-cause projection is still more pessimistic for younger ages, but the life expectancy at 60 years is equivalent between the two models.

Figures 22 and 23 plot the life expectancy of central projections with the Lee-Carter model, with a by-cause projection and with an all-causes projection.

Figure 22

COMPARISON OF THE ALL-CAUSE AND THE BY-CAUSE–LIFE EXPECTANCY AT BIRTH

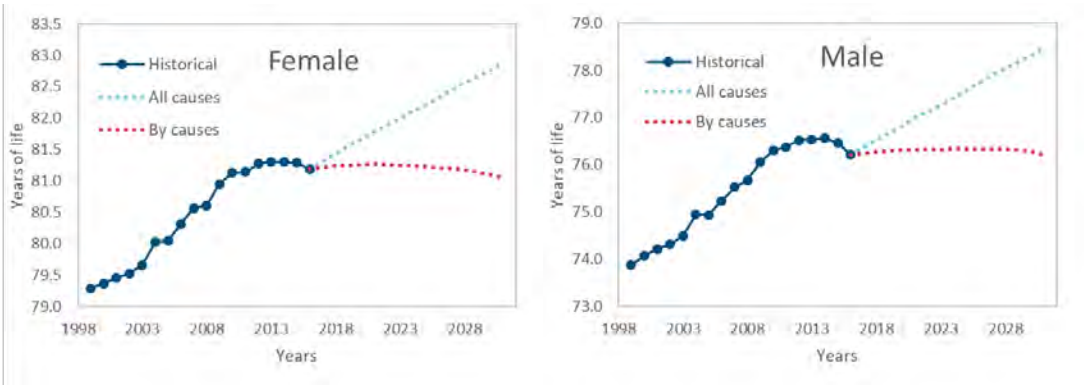

Figure 23

COMPARISON OF THE ALL-CAUSE AND THE BY-CAUSE–LIFE EXPECTANCY AT 60 YEARS OLD

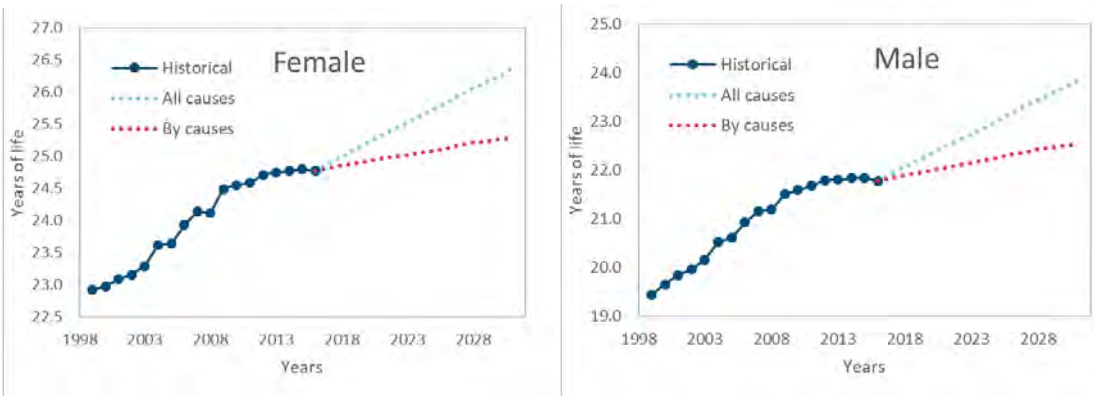

The cause-based forecast is again more pessimistic than the aggregate projection. This is mainly explained by the projected increase of drug and dementia causes following the historical trend. From a forecasting perspective, the by-cause model allows one to recover interesting projections, in particular more in line with the recent experience. To this extent, the authors argue that they seem more plausible when compared to an aggregate forecast. The forecast of drug causes explains why the pessimism of the by-cause model is more marked when looking at the life expectancy at birth. However, the pessimism of the by-cause model is also partly explained by the fact no breakpoint has been used for the all-cause projection. Section 7 of the Appendix shows that when using breakpoint for by-cause projection the two models forecast similar life expectancies at age 60.

The average projected yearly life expectancy improvements at ages 0, 40, 60 and 80 (in months) are given in Tables 8 and 9.

Table 8

AVERAGE YEARLY IMPROVEMENT IN LIFE EXPECTANCY (IN MONTHS) FOR BY-CAUSE OR ALL-CAUSES FORECASTS, FEMALE

	0	40	60	80
By-cause	−0.1	0.2	0.4	0.2
All-causes	1.4	1.3	1.3	0.8

Table 9

AVERAGE YEARLY IMPROVEMENT IN LIFE EXPECTANCY (IN MONTHS) FOR BY-CAUSE OR ALL-CAUSES FORECASTS, MALE

	0	40	60	80
By-cause	−0.0	0.5	0.6	0.3
All-causes	1.8	1.7	1.6	1.0

Section 7: Acknowledgements

The researchers would like to thank the Project Oversight Group for their guidance and feedback on the report.

Project Oversight Group Members:

Jim Filmore, Chairperson

Mary Pat Campbell

Henry Egesi

Sophie Feng

Jean-Marc Fix

Blake Hill

Jason McKinley

Larry Stern

Mark Walker

Daniel Zamarripa

At the Society of Actuaries:

R. Dale Hall, Managing Director of Research

Jan Schuh, Senior Research Administrator

Ronora Stryker, Senior Practice Research Actuary

Appendix

1. HCD INTERMEDIATE LIST

The HCD intermediate list is detailed in Table 10, along with the corresponding ICD 10 classification codes.

Table 10

HCD INTERMEDIATE LIST

No.	Title	Category codes according to ICD10
0	All causes	A00–Y98
1	Other specified intestinal infections	A00–A08
2	Diarrhea and gastroenteritis of presumed infectious origin	A09
3	TBC	A15–A19, B90
4	Septicemia	A40–A41
5	Other bacterial diseases	A20–A28, A30–A39 A42–A44, A46, A48–A49
6	HIV disease	B20–B24
7	Viral hepatitis	B15–B19
8	Other viral diseases	A80-A89, B00-B09, B25–B34
9	Other and unspecified infectious and parasitic diseases	A50–A75, A77–A79, A90–A99, B35–B60, B64–B89, B91, B92, B94–B97, B99
10	Malignant neoplasms of lip, oral cavity and pharynx	C00–C14
11	Malignant neoplasm of esophagus	C15
12	Malignant neoplasm of stomach	C16
13	Malignant neoplasms of colon	C18
14	Malignant neoplasm of rectum and anus	C19–C21
15	Malignant neoplasms of liver and intrahepatic bile ducts	C22
16	Malignant neoplasm of pancreas	C25
17	Other malignant neoplasm of digestive system	C17, C23–C24, C26
18	Malignant neoplasm of larynx	C32
19	Malignant neoplasms of trachea, bronchus and lung	C33-C34
20	Malignant neoplasm of skin	C43, C44
21	Malignant neoplasm of breast	C50
22	Malignant neoplasm of cervix uteri	C53
23	Malignant neoplasms of uterus	C54–C55
24	Malignant neoplasm of ovary	C56
25	Malignant neoplasm of prostate	C61
26	Malignant neoplasm of other genital organs	C51, C52, C57, C58, C60, C62, C63
27	Malignant neoplasm of bladder	C67
28	Malignant neoplasms of kidney and other urinary organ	C64–C66, C68
29	Malignant neoplasms of meninges, brain and other parts of central nervous system	C70-C72
30	Leukemia	C91–C95
31	Other malignant neoplasms of lymphoid, hematopoietic and related tissue	Other malignant neoplasms of lymphoid, hematopoietic and related tissue
32	Malignant neoplasms of independent (primary) multiple sites	C97
33	Other cancer	C30–C31,C37–C41, C45–C49, C69, C73–C80
34	In situ neoplasms, benign neoplasms and neoplasms of uncertain or unknown behavior	D00–D48
35	Diabetes mellitus	E10–E14
36	Malnutrition	E40–E46
37	Other endocrinologic and metabolic diseases	E00–E07, E15–E16, E20–E35, E50–E68, E70–E90
38	Blood diseases	D50–D89
39	Dementia, vascular, senile or unspecified	F01, F03
40	Alcohol abuse	F10
41	Drug abuse	F11-F19
42	Other mental disorders	F04–F09, F20–F99

43	Systemic atrophies and demyelinating diseases of the central nervous system	G10–G12, G35–G37
44	Parkinson's disease and other extrapyramidal and movement disorders	G20–G25
45	Alzheimer's disease and other degenerative diseases of the nervous system	G30, G31
46	Epilepsy	G40–G41
47	Other diseases of nervous system	G00–G09, G43–G44, G47–G83, G90–G99, H00–H95
48	Rheumatic heart diseases	I00–I09
49	Essential hypertension	I10
50	Hypertensive disease (heart, kidney and secondary)	I11–I15
51	Acute myocardial infarction	I21–I23
52	Atherosclerotic cardiovascular and heart diseases	I25.0, I25.1
53	Other IHD	I20, I24, I25.2 to .9
54	Pulmonary heart diseases	I26–I28
55	Non rheumatic valve disorders	I34–I38
56	Cardiac arrest	I46
57	Heart failure	I50
58	Other heart diseases	I30–I33, I40–I45, I47–I49, I51
59	Intracranial hemorrhage	I60–I62
60	Cerebral infarction, occlusion, and stenosis	I63, I65, I66
61	Other cerebrovascular diseases	G45, I64, I67
62	Sequelae of cerebrovascular disease	I69
63	Diseases of arteries, arterioles and capillaries	I70–I78
64	Other circulatory diseases	I80–I99
65	Influenza	J09–J11
66	Pneumonia	J12–J18
67	Other acute respiratory infections	J00–J06, J20–J22, U04
68	Asthma	J45–J46
69	Other chronic obstructive pulmonary disease	J40–J44, J47
70	Pneumonitis due to solids and liquids	J69
71	Pneumoconiosis and chemical effects	J60–J68, J70
72	Other respiratory diseases, principally affecting the interstitium	J80–J84
73	Other diseases of the respiratory system	J30–J39, J85–J98
74	Gastric and duodenal ulcer	K25–K28
75	Hernia	K40–K46
76	Enteritis, colitis and other intestinal diseases	K35–K38, K50–K63
77	Alcoholic cirrhoses of liver	K70
78	Other cirrhoses of liver	K74
79	Other diseases of liver	K71–K73, K75, K76
80	Cholelithiasis and other disorders of biliary tracts	K80–K83
81	Diseases of pancreas	K85–K86
82	Other digestive diseases	K00–K22, K29–K31, K65–K66, K90–K92
83	Diseases of skin and subcutaneous tissue	L00–L98
84	Diseases of the musculoskeletal system and connective tissue	M00–M99
85	Renal tubulo-interstitial diseases	N00–N15
86	Renal failure	N17–N19
87	Other diseases of urinary system	N20–N36, N39
88	Diseases of genital organs	N40–N99
89	Complications of pregnancy, childbirth, and puerperium	O00–O99
90	Certain conditions originating in the perinatal period	P00–P96
91	Congenital malformations, deformations, and chromosomal abnormalities	Q00–Q99
92	Sudden infant death syndrome (SIDS)	R95
93	Transport accidents	V01–V99
94	Accidental falls	W00–W19
95	Accidental drowning and submersion	W65–W74
96	Accidental exposure to smoke, fire and flames	X00–X09
97	Accidental poisoning by alcohol	X45
98	Accidental poisoning by other substance	X40–X44, X46–X49
99	Other accidental threats to breathing	W75–W84
100	Suicide and self-inflicted injury	X60–X84
101	Assault	X85–Y09, Y35, Y36
102	Event of undetermined intent	Y10–Y34

103	Complications of medical and surgical care	Y40–Y84
104	Other accidents and late effects of accidents (remainder)	W20–W64, W85–W99, X10–X39, X50–X59, Y85–Y91, Y95–Y98

2. CAUSE MAPPING

Table 11 shows the mapping between defined causes and HCD/GBD lists.

Table 11
CAUSES MAPPING

Cause of Death	GBD Classification	HCD Classification
Cardiovascular diseases (A)	B.2.1 Rheumatic heart disease B.2.2 Ischemic heart disease B.2.5 Non-rheumatic valvular heart disease B.2.6 Cardiomyopathy and myocarditis B.2.7 Atrial fibrillation and flutter B.2.8 Aortic aneurysm B.2.9 Peripheral artery disease B.2.10 Endocarditis B.2.11 Other cardiovascular and circulatory diseases	Rheumatic heart diseases Essential hypertension Acute myocardial infarction Atherosclerotic cardiovascular and heart diseases Other IHD Pulmonary heart diseases Non rheumatic valve disorders Cardiac arrest Heart failure Other heart diseases Diseases of arteries, arterioles and capillaries Other circulatory diseases
Cerebrovascular diseases (B)	B.2.3. Stroke	Intracranial hemorrhage Cerebral infarction, occlusion, and stenosis Other Cerebrovascular Sequelae of cerebrovascular disease
Neoplasms directly induced by smoking (NeoSmok, C)	B.1.1 Lip and oral cavity cancer B.1.2 Nasopharynx cancer B.1.3 Other pharynx cancer B.1.10 Larynx cancer B.1.11 Tracheal, bronchus, and lung cancer	Malignant Neoplasm of lip, oral cavity and pharynx Malignant neoplasm of larynx Malignant Neoplasm of trachea, bronchus and lung
Neoplasms not directly induced by smoking (D)	B.1.4 Esophageal cancer B.1.5 Stomach cancer B.1.6 Colon and rectum cancer B.1.7 Liver cancer B.1.8 Gallbladder and biliary tract cancer B.1.9 Pancreatic cancer B.1.12 Malignant skin melanoma B.1.13 Non-melanoma skin cancer B.1.14 Breast cancer B.1.15 Cervical cancer B.1.16 Uterine cancer B.1.17 Ovarian cancer B.1.18 Prostate cancer B.1.19 Testicular cancer B.1.20 Kidney cancer B.1.21 Bladder cancer B.1.22 Brain and nervous system cancer B.1.23 Thyroid cancer B.1.24 Mesothelioma B.1.25 Hodgkin lymphoma B.1.26 Non-Hodgkin lymphoma B.1.27 Multiple myeloma B.1.28 Leukemia	Malignant neoplasm of esophagus Malignant neoplasm of stomach Malignant Neoplasm of colon Malignant neoplasm of rectum and anus Malignant Neoplasm of liver and intrahepatic bile ducts Malignant neoplasm of pancreas Other malignant neoplasm of digestive system Malignant neoplasm of skin Malignant neoplasm of breast Malignant neoplasm of cervix uteri Malignant Neoplasm of uterus Malignant neoplasm of ovary Malignant neoplasm of prostate Malignant neoplasm of other genital organs Malignant neoplasm of bladder Malignant Neoplasm of kidney and other urinary organ Malignant Neoplasm of meninges, brain and other parts of central nervous system Leukemia

	B.1.29 Other malignant Neoplasm B.1.30 Other Neoplasm	Other malignant Neoplasm of lymphoid, hematopoietic and related tissue Malignant Neoplasm of independent (primary) multiple sites Other cancer In situ Neoplasm, benign Neoplasm and Neoplasm of uncertain or unknown behavior
Dementia (E)	B.5.1 Alzheimer's disease and other dementias B.5.2 Parkinson's disease	Dementia, vascular, senile or unspecified Parkinson's disease and other extrapyramidal and movement disorders Alzheimer's disease and other degenerative diseases of the nervous system
Diabetes (F)	B.2.4 Hypertensive heart disease B.8.1 Diabetes mellitus B.8.2 Chronic kidney disease	Diabetes mellitus Hypertensive disease (heart, kidney and secondary) Renal failure
Influenza (G)	A.2.2 Lower respiratory infections A.2.3 Upper respiratory infections	Influenza Pneumonia Other acute respiratory infections
Respiratory diseases (H)	A.2.1 Tuberculosis B.3.1 Chronic obstructive pulmonary disease B.3.2 Pneumoconiosis B.3.3 Asthma B.3.4 Interstitial lung disease and pulmonary sarcoidosis B.3.5 Other chronic respiratory diseases	Asthma Other chronic obstructive pulmonary disease Pneumonitis due to solids and liquids Pneumoconiosis and chemical effects Other Respiratory, principally affecting the interstitium Other diseases of the respiratory system
Drug abuse (I)	B.2.4 Hypertensive heart disease B.8.1 Diabetes mellitus B.8.2 Chronic kidney disease	Alcohol abuse Drug abuse Alcoholic cirrhosis of liver Accidental poisoning by alcohol Accidental poisoning by other substance
External causes (J)	C.1.1 Road injuries C.1.2 Other transport injuries C.2.1 Falls C.2.2 Drowning C.2.3 Fire, heat, and hot substances C.2.4 Poisonings C.2.5 Exposure to mechanical forces C.2.6 Adverse effects of medical treatment C.2.7 Animal contact C.2.8 Foreign body C.2.9 Environmental heat and cold exposure C.2.10 Exposure to forces of nature C.2.11 Other unintentional injuries C.3.1 Self-harm C.3.2 Interpersonal violence C.3.3 Conflict and terrorism C.3.4 Executions and police conflict	Transport accidents Accidental falls Accidental drowning and submersion Accidental exposure to smoke, fire and flames Other accidental threats to breathing Suicide and self-inflicted injury Assault Event of undetermined intent Complications of medical and surgical care Other accidents and late effects of accidents (remainder)
Other (K)	A.1.1 HIV/AIDS A.1.2 Sexually transmitted infections excluding HIV A.2.4 Otitis media A.3.1 Diarrheal diseases A.3.2 Typhoid and paratyphoid	Other specified intestinal infections Diarrhea and gastroenteritis of presumed infectious origin TBC Septicemia Other bacterial diseases

	A.3.3 Invasive Non-typhoidal Salmonella (iNTS) A.3.5 Other intestinal infectious diseases A.4.1 Malaria A.4.2 Chagas disease A.4.3 Leishmaniasis A.4.4 African trypanosomiasis A.4.5 Schistosomiasis A.4.6 Cysticercosis A.4.7 Cystic echinococcosis A.4.8 Lymphatic filariasis A.4.9 Onchocerciasis A.4.10 Trachoma A.4.11 Dengue A.4.12 Yellow fever A.4.13 Rabies A.4.14 Intestinal nematode infections A.4.15 Food-borne trematodiases A.4.16 Leprosy A.4.17 Ebola A.4.18 Zika virus A.4.19 Guinea worm disease A.4.20 Other neglected tropical diseases A.5.1 Meningitis A.5.2 Encephalitis A.5.3 Diphtheria A.5.4 Whooping cough A.5.5 Tetanus A.5.6 Measles A.5.7 Varicella and herpes zoster A.5.8 Acute hepatitis A.5.9 Other unspecified infectious diseases A.6.1 Maternal disorders A.6.2 Neonatal disorders A.7.1 Protein-energy malnutrition A.7.2 Iodine deficiency A.7.3 Vitamin A deficiency A.7.4 Dietary iron deficiency A.7.5 Other nutritional deficiencies B.4.2 Upper digestive system diseases B.4.3 Appendicitis B.4.4 Paralytic ileus and intestinal obstruction B.4.5 Inguinal, femoral, and abdominal hernia B.4.6 Inflammatory bowel disease B.4.7 Vascular intestinal disorders B.4.8 Gallbladder and biliary diseases B.4.9 Pancreatitis B.4.10 Other digestive diseases B.5.3 Epilepsy B.5.4 Multiple sclerosis B.5.5 Motor neuron disease B.5.6 Headache disorders B.5.7 Other neurological disorders B.6.1 Schizophrenia B.6.2 Depressive disorders B.6.3 Bipolar disorder B.6.4 Anxiety disorders B.6.5 Eating disorders	HIV disease Viral hepatitis Other viral diseases Other and unspecified infectious and parasitic disease Malnutrition Other endocrinologic and metabolic diseases Blood diseases Other mental disorders Systemic atrophies and demyelinating diseases of the central nervous system Epilepsy Other diseases of nervous system Gastric and duodenal ulcer Hernia Enteritis, colitis and other intestinal diseases Other cirrhoses of liver Other diseases of liver Cholelithiasis and other disorders of biliary tracts Diseases of pancreas Other digestive diseases Diseases of skin and subcutaneous tissue Diseases of the musculoskeletal system and connective tissue Renal tubulo-interstitial diseases Other diseases of urinary system Diseases of genital organs Complications of pregnancy, childbirth, and puerperium Certain conditions originating in the perinatal period Congenital malformations, deformations, and chromosomal abnormalities Sudden infant death syndrome (SIDS)

	B.6.6 Autism spectrum disorders B.6.7 Attention-deficit/hyperactivity disorder B.6.8 Conduct disorder B.6.9 Idiopathic developmental intellectual disability B.6.10 Other mental disorders B.8.3 Acute glomerulonephritis B.9.1 Dermatitis B.9.2 Psoriasis B.9.3 Bacterial skin diseases B.9.4 Scabies B.9.5 Fungal skin diseases B.9.6 Viral skin diseases B.9.7 Acne vulgaris B.9.8 Alopecia areata B.9.9 Pruritus B.9.10 Urticaria B.9.11 Decubitus ulcer B.9.12 Other skin and subcutaneous diseases B.10.1 Blindness and vision impairment B.10.2 Age-related and other hearing loss B.10.3 Other sense organ diseases B.11.1 Rheumatoid arthritis B.11.2 Osteoarthritis B.11.3 Low back pain B.11.4 Neck pain B.11.5 Gout B.11.6 Other musculoskeletal disorders B.12.1 Congenital birth defects B.12.2 Urinary diseases and male infertility B.12.3 Gynecological diseases B.12.4 Hemoglobinopathies and hemolytic anemias B.12.5 Endocrine, metabolic, blood, and immune disorders B.12.6 Oral disorders B.12.7 Sudden infant death syndrome	

3. MERGING OF THE HCD AND GBD DATABASES

To match the two databases (HCD and GBD), the authors compared the number of deaths for each cause between the two tables. For 1999–2013, HCD data are considered as the reference. For 2014–2017, the authors adjusted the GBD data so that 2013 HCD deaths remain unchanged.

The charts below show the number of deaths in 2013 for the two databases. The numbers of deaths are very similar between the HCD data and GBD data, but an adjustment is needed to reconcile the 2013 death levels. The numbers of deaths are given by age group in Figure 24.

Figure 24
NUMBER OF DEATHS BY CAUSE IN 2013 IN HCD AND GBD TABLES

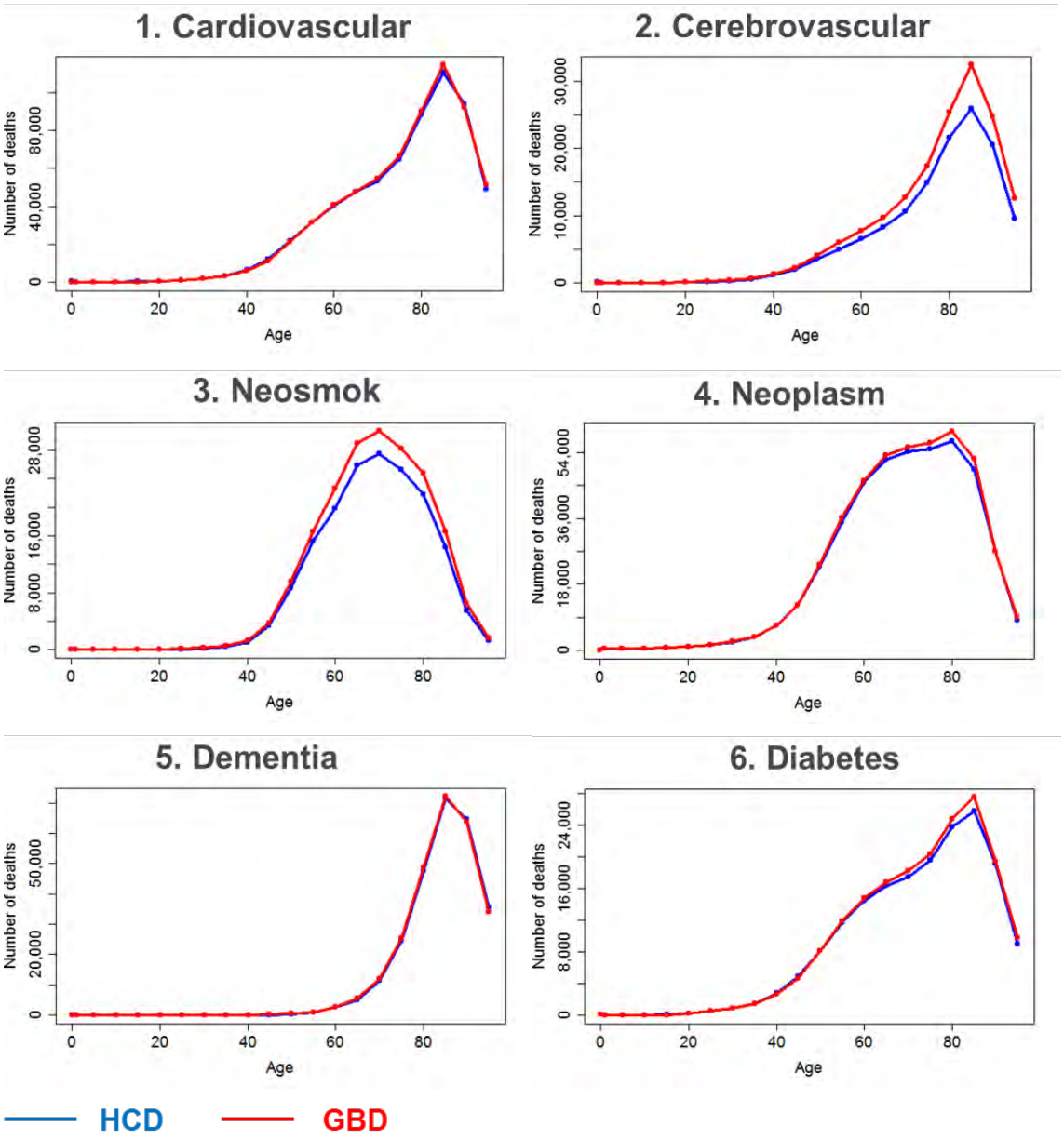

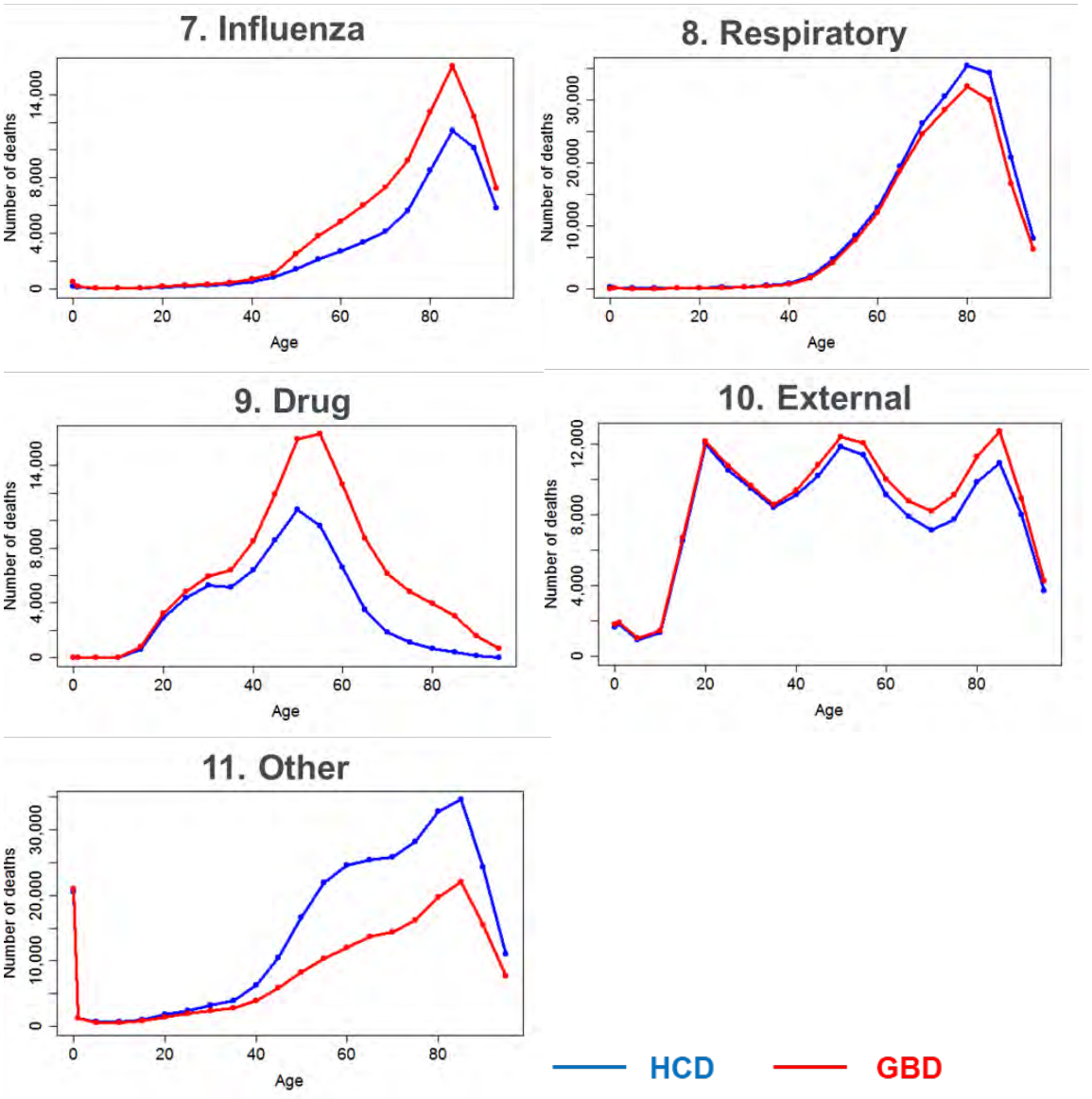

The numbers of deaths are close for each cause. The discrepancy observed for drug causes is explained by inclusion of "Cirrhosis and other chronic liver diseases " in GBD while only "Alcoholic cirrhosis of liver" is included in HCD. Alcoholic cirrhosis is not separable from other cirrhosis on the GBD intermediate list.

4. FITTED PARAMETERS OF THE LEE-CARTER MODEL

Table 12 shows the fitted parameters of the Lee-Carter model.

Table 12

LEE-CARTER FITTED α_x, MALE

	Cardio.	Cerebro.	NeoSmok	Neoplasm	Dementia	Diabetes	Influenza	Resp.	Drug	External	Other
0	−9.02	−10.27	−14.67	−10.30	−12.63	−10.20	−9.34	−9.27	−12.60	−7.72	−5.06
1–4	−11.28	−12.60	−15.98	−10.41	−13.40	−13.78	−11.52	−11.38	−12.91	−8.78	−9.28
5–9	−12.26	−13.15	−15.97	−10.49	−14.39	−14.23	−12.68	−12.11	−14.17	−9.63	−10.22
10–14	−11.76	−12.95	−15.21	−10.55	−14.57	−13.33	−12.79	−11.98	−13.14	−9.19	−10.15
15–19	−10.67	−12.56	−14.11	−10.15	−14.75	−12.36	−12.43	−11.84	−9.98	−7.43	−9.70
20–24	−10.04	−12.00	−13.19	−9.82	−14.48	−11.25	−11.83	−11.39	−8.78	−6.95	−9.32
25–29	−9.49	−11.48	−12.57	−9.52	−14.40	−10.55	−11.54	−11.19	−8.46	−7.08	−9.00
30–34	−8.89	−10.86	−11.71	−9.15	−14.05	−9.84	−11.19	−10.94	−8.31	−7.21	−8.61
35–39	−8.27	−10.22	−10.59	−8.70	−13.56	−9.28	−10.86	−10.54	−8.10	−7.25	−8.18
40–44	−7.60	−9.58	−9.42	−8.12	−12.91	−8.70	−10.39	−10.00	−7.84	−7.23	−7.75
45–49	−7.00	−9.02	−8.37	−7.45	−12.03	−8.19	−9.97	−9.27	−7.61	−7.19	−7.32
50–54	−6.47	−8.54	−7.55	−6.82	−11.15	−7.73	−9.53	−8.52	−7.55	−7.18	−6.98
55–59	−6.02	−8.10	−6.89	−6.28	−10.12	−7.31	−9.14	−7.79	−7.63	−7.20	−6.75
60–64	−5.60	−7.63	−6.36	−5.82	−9.06	−6.92	−8.67	−7.09	−7.79	−7.22	−6.54
65–69	−5.22	−7.15	−5.90	−5.42	−8.04	−6.57	−8.17	−6.44	−8.03	−7.15	−6.28
70–74	−4.79	−6.57	−5.56	−5.03	−6.94	−6.19	−7.55	−5.83	−8.25	−6.92	−5.93
75–79	−4.30	−5.95	−5.34	−4.66	−5.92	−5.76	−6.87	−5.32	−8.39	−6.55	−5.51
80–84	−3.73	−5.33	−5.19	−4.28	−5.01	−5.27	−6.11	−4.85	−8.56	−6.07	−5.04
85–89	−3.13	−4.74	−5.16	−3.95	−4.25	−4.77	−5.37	−4.42	−8.61	−5.56	−4.54
90–94	−2.52	−4.20	−5.21	−3.65	−3.61	−4.26	−4.61	−4.03	−8.68	−5.07	−4.03
95+	−1.95	−3.75	−5.32	−3.43	−3.10	−3.78	−3.84	−3.64	−8.72	−4.61	−3.53

Table 13

LEE-CARTER FITTED $\beta_x \times 100$, MALE

	Cardio.	Cerebro.	NeoSmok	Neoplasm	Dementia	Diabetes	Influenza	Resp.	Drug	External	Other
0	5.04	1.36	2.15	3.63	−15.18	36.10	12.22	4.40	−53.94	−5.99	5.96
1–4	2.34	−0.18	25.00	6.13	−18.25	27.23	4.05	−6.37	−2.35	10.15	8.47
5–9	5.30	−1.85	2.14	4.22	−8.29	29.48	−5.94	−20.75	−13.13	23.56	3.35
10–14	7.12	−3.44	3.14	5.58	−6.90	21.10	−6.52	11.29	−16.03	21.62	7.86
15–19	3.93	2.64	6.77	5.90	−20.69	9.85	0.38	27.91	14.44	21.14	5.34
20–24	1.07	3.96	0.53	6.75	−8.46	−5.30	−1.89	0.68	30.92	12.22	1.57
25–29	−0.59	3.00	1.63	1.46	−0.78	−8.73	−7.52	−8.47	39.13	6.39	3.44
30–34	0.06	1.04	2.55	2.72	11.39	−8.74	−5.77	−1.37	37.50	3.68	10.55
35–39	2.30	2.68	6.86	4.44	−4.00	−9.43	2.30	2.69	19.24	6.32	16.59
40–44	4.08	3.91	9.67	6.23	3.85	−7.54	4.73	10.80	7.46	8.15	14.02
45–49	4.47	4.24	6.27	6.14	8.99	−5.70	4.31	6.32	8.58	4.02	8.85
50–54	4.02	3.36	3.74	3.46	13.50	−5.91	0.31	−7.52	18.18	−3.41	1.62
55–59	4.69	3.33	3.94	2.08	15.20	−5.15	−3.93	−0.37	24.64	−6.43	−4.91
60–64	5.83	5.38	5.14	3.05	16.72	−2.19	1.96	6.96	21.36	−3.48	−5.24
65–69	7.31	7.64	4.81	5.11	13.69	3.86	5.91	11.86	8.67	−1.12	−1.06
70–74	8.29	8.93	4.19	5.57	14.03	6.66	10.13	11.43	2.83	1.00	1.14
75–79	8.30	9.81	3.40	5.43	14.63	7.63	13.54	11.16	2.56	2.55	2.13
80–84	8.39	11.34	2.58	5.94	14.32	8.92	17.34	12.31	−1.75	1.80	3.99
85–89	7.80	12.66	2.23	6.58	14.93	9.69	18.93	13.44	−3.59	2.41	5.64
90–94	5.91	11.31	1.77	5.10	18.45	2.67	18.73	9.65	−14.45	0.06	5.48
95+	4.35	8.86	1.47	4.47	22.84	−4.49	16.72	3.96	−30.26	−4.65	5.19

Table 14

LEE-CARTER FITTED κ_t, MALE

	Cardio.	Cerebro.	NeoSmok	Neoplasm	Dementia	Diabetes	Influenza	Resp.	Drug	External	Other
1999	4.53	3.67	4.99	2.67	−2.66	0.85	2.04	1.28	−1.61	1.00	2.19
2000	4.01	3.48	4.90	2.32	−2.26	0.84	2.05	0.95	−1.55	1.00	1.98
2001	3.42	3.02	4.44	1.99	−1.80	0.85	1.60	0.75	−1.43	1.15	1.80
2002	3.07	2.69	3.76	1.72	−1.48	0.90	1.82	0.68	−1.06	1.00	1.89
2003	2.49	2.22	3.26	1.24	−1.19	0.91	1.53	0.47	−0.79	0.85	1.55
2004	1.50	1.48	2.59	0.72	−1.15	0.69	0.94	0.16	−0.65	0.68	1.13
2005	1.13	0.79	2.11	0.57	−0.60	0.66	1.00	0.29	−0.30	0.73	1.02
2006	0.30	0.04	1.22	0.11	0.15	0.28	0.25	−0.20	0.08	0.67	0.52
2007	−0.42	−0.35	0.34	−0.04	0.14	0.03	−0.37	−0.22	0.09	0.42	0.28
2008	−0.81	−0.70	−0.28	−0.34	0.72	−0.17	−0.33	0.15	0.20	−0.09	−0.13
2009	−1.45	−1.35	−1.16	−0.64	0.59	−0.68	−1.06	−0.34	0.19	−0.65	−0.57
2010	−1.88	−1.58	−1.81	−0.81	1.00	−0.60	−1.27	−0.37	0.32	−0.85	−0.97
2011	−2.28	−1.90	−2.58	−1.17	1.25	−0.56	−1.15	−0.37	0.59	−0.91	−1.40
2012	−2.57	−2.17	−3.33	−1.45	1.38	−0.74	−1.59	−0.62	0.64	−0.98	−1.80
2013	−2.64	−2.30	−4.30	−1.71	1.45	−0.72	−1.33	−0.55	0.89	−1.23	−1.77
2014	−2.80	−2.36	−4.72	−1.81	1.48	−0.79	−1.39	−0.65	1.14	−1.22	−1.91
2015	−2.87	−2.37	−5.01	−1.82	1.49	−0.84	−1.39	−0.68	1.46	−0.95	−1.99

Table 15

LEE-CARTER FITTED α_x, FEMALE

	Cardio.	Cerebro.	NeoSmok	Neoplasm	Dementia	Diabetes	Influenza	Resp.	Drug	External	Other
0	−9.18	−10.49	−15.98	−10.32	−12.88	−10.53	−9.69	−9.55	−12.82	−7.98	−5.25
1–4	−11.38	−12.71	−16.04	−10.54	−13.54	−13.88	−11.56	−11.67	−13.25	−9.15	−9.38
5–9	−12.23	−13.19	−15.72	−10.63	−14.42	−14.13	−12.74	−12.47	−14.23	−9.98	−10.32
10–14	−12.01	−13.02	−15.32	−10.65	−14.71	−13.39	−12.77	−12.22	−13.43	−9.80	−10.27
15–19	−11.24	−12.73	−14.61	−10.48	−14.88	−12.62	−12.60	−12.13	−11.04	−8.49	−9.92
20–24	−10.62	−12.14	−13.58	−10.15	−14.90	−11.61	−12.10	−11.79	−9.93	−8.36	−9.40
25–29	−10.09	−11.62	−12.93	−9.64	−14.49	−10.85	−11.76	−11.42	−9.52	−8.46	−9.09
30–34	−9.58	−10.97	−11.97	−8.99	−14.19	−10.31	−11.45	−11.07	−9.19	−8.48	−8.79
35–39	−9.03	−10.37	−10.78	−8.36	−13.58	−9.80	−11.03	−10.58	−8.84	−8.39	−8.48
40–44	−8.46	−9.70	−9.61	−7.79	−13.13	−9.27	−10.63	−9.99	−8.54	−8.30	−8.14
45–49	−7.93	−9.21	−8.68	−7.28	−12.17	−8.75	−10.28	−9.29	−8.34	−8.23	−7.78
50–54	−7.44	−8.81	−7.99	−6.81	−11.31	−8.26	−9.93	−8.62	−8.40	−8.23	−7.46
55–59	−6.95	−8.43	−7.41	−6.40	−10.25	−7.79	−9.53	−7.97	−8.62	−8.24	−7.16
60–64	−6.44	−7.97	−6.89	−6.01	−9.27	−7.35	−9.05	−7.32	−8.90	−8.21	−6.84
65–69	−5.94	−7.43	−6.42	−5.68	−8.29	−6.92	−8.57	−6.68	−9.15	−8.06	−6.48
70–74	−5.40	−6.79	−6.08	−5.35	−7.16	−6.47	−7.94	−6.12	−9.36	−7.74	−6.08
75–79	−4.80	−6.09	−5.88	−5.04	−6.05	−6.03	−7.25	−5.66	−9.48	−7.26	−5.63
80–84	−4.14	−5.37	−5.81	−4.74	−5.06	−5.54	−6.49	−5.25	−9.54	−6.69	−5.15
85–89	−3.44	−4.71	−5.86	−4.47	−4.21	−5.02	−5.74	−4.89	−9.52	−6.12	−4.63
90–94	−2.77	−4.13	−6.00	−4.28	−3.49	−4.52	−5.00	−4.58	−9.57	−5.57	−4.13
95+	−2.11	−3.65	−6.17	−4.15	−2.84	−4.01	−4.24	−4.25	−9.49	−5.04	−3.61

Table 16

LEE-CARTER FITTED $\beta_x \times 100$, FEMALE

	Cardio.	Cerebro.	NeoSmok	Neoplasm	Dementia	Diabetes	Influenza	Resp.	Drug	External	Other
0	6.89	−1.54	−13.84	5.36	−18.78	18.65	23.21	12.33	−10.54	−5.44	6.97
1–4	2.14	5.15	36.80	4.67	−25.35	11.84	7.58	−58.31	−2.30	16.60	7.98
5–9	3.42	−6.16	−5.77	5.28	−28.00	7.78	−9.23	−119.95	−5.63	30.58	6.87
10–14	5.88	0.88	6.37	2.77	−15.83	13.21	−4.37	−25.02	−2.89	23.34	8.97
15–19	4.85	1.77	12.19	5.23	−16.58	8.24	0.45	177.53	8.16	28.95	8.34
20–24	3.80	6.42	4.89	6.02	−16.64	3.84	−2.65	149.55	16.01	10.04	5.01
25–29	1.64	3.63	−2.87	5.04	10.77	−0.32	−16.56	101.76	19.18	4.23	5.36
30–34	0.82	3.32	7.54	3.99	0.98	−1.55	−13.39	89.14	16.41	5.00	5.53
35–39	1.80	5.78	15.49	5.16	11.29	−2.10	−0.16	17.89	9.46	11.47	7.46
40–44	2.44	6.08	13.52	5.04	6.10	−1.66	−2.63	75.53	7.10	10.19	7.93
45–49	1.99	5.11	6.16	5.29	12.30	−1.54	−2.32	−89.88	9.80	1.57	2.42
50–54	2.53	3.37	1.64	4.83	18.89	0.19	−7.85	−169.79	14.44	−5.60	−2.78
55–59	4.49	4.80	4.63	5.15	16.78	2.72	−5.15	−46.91	14.22	−7.60	−4.47
60–64	6.55	6.01	8.31	5.21	17.88	5.24	2.24	89.02	9.91	0.40	−2.20
65–69	7.66	7.11	5.90	5.44	14.94	8.04	4.55	67.21	5.36	3.07	−0.81
70–74	7.86	7.66	3.55	5.01	15.97	6.94	11.10	19.03	1.42	3.93	1.01
75–79	7.73	7.63	1.66	4.50	17.40	6.51	15.88	−2.55	−0.38	0.85	2.07
80–84	7.84	8.48	−0.00	4.66	17.24	5.80	21.57	−13.85	−1.41	−2.11	5.59
85–89	7.53	8.86	−1.12	4.65	17.94	4.98	25.66	−20.89	−3.10	−5.27	8.63
90–94	6.53	8.23	−1.76	3.66	19.72	3.10	26.29	−64.14	−2.40	−9.19	9.94
95+	5.62	7.40	−3.28	3.04	22.98	0.10	25.77	−87.70	−2.84	−15.00	10.18

Table 17

LEE-CARTER FITTED κ_t, FEMALE

	Cardio.	Cerebro.	NeoSmok	Neoplasm	Dementia	Diabetes	Influenza	Resp.	Drug	External	Other
1999	6.89	−1.54	−13.84	5.36	−18.78	18.65	23.21	12.33	−10.54	−5.44	6.97
2000	2.14	5.15	36.80	4.67	−25.35	11.84	7.58	−58.31	−2.30	16.60	7.98
2001	3.42	−6.16	−5.77	5.28	−28.00	7.78	−9.23	−119.95	−5.63	30.58	6.87
2002	5.88	0.88	6.37	2.77	−15.83	13.21	−4.37	−25.02	−2.89	23.34	8.97
2003	4.85	1.77	12.19	5.23	−16.58	8.24	0.45	177.53	8.16	28.95	8.34
2004	3.80	6.42	4.89	6.02	−16.64	3.84	−2.65	149.55	16.01	10.04	5.01
2005	1.64	3.63	−2.87	5.04	10.77	−0.32	−16.56	101.76	19.18	4.23	5.36
2006	0.82	3.32	7.54	3.99	0.98	−1.55	−13.39	89.14	16.41	5.00	5.53
2007	1.80	5.78	15.49	5.16	11.29	−2.10	−0.16	17.89	9.46	11.47	7.46
2008	2.44	6.08	13.52	5.04	6.10	−1.66	−2.63	75.53	7.10	10.19	7.93
2009	1.99	5.11	6.16	5.29	12.30	−1.54	−2.32	−89.88	9.80	1.57	2.42
2010	2.53	3.37	1.64	4.83	18.89	0.19	−7.85	−169.79	14.44	−5.60	−2.78
2011	4.49	4.80	4.63	5.15	16.78	2.72	−5.15	−46.91	14.22	−7.60	−4.47
2012	6.55	6.01	8.31	5.21	17.88	5.24	2.24	89.02	9.91	0.40	−2.20
2013	7.66	7.11	5.90	5.44	14.94	8.04	4.55	67.21	5.36	3.07	−0.81
2014	7.86	7.66	3.55	5.01	15.97	6.94	11.10	19.03	1.42	3.93	1.01
2015	7.73	7.63	1.66	4.50	17.40	6.51	15.88	−2.55	−0.38	0.85	2.07

The quantity $\beta_x \times \Delta$ is given by age and cause of death, which corresponds to the trend by age and cause, or the relative yearly deviation of mortality central projections (log base).

Table 18

BY-CAUSE MODEL TREND BY AGE ($\beta_x \times 100 \times \Delta$), MALE

	Cardio.	Cerebro.	NeoSmok	Neoplasm	Dementia	Diabetes	Influenza	Resp.	Drug	External	Other
0	−0.72	−0.19	−1.19	−0.47	−1.46	−1.20	−0.49	−0.52	−10.82	−0.26	−1.40
1–4	−0.33	0.02	−13.86	−0.79	−1.75	−0.90	−0.16	0.75	−0.47	0.43	−1.99
5–9	−0.76	0.25	−1.19	−0.54	−0.80	−0.98	0.24	2.45	−2.63	1.00	−0.79
10–14	−1.02	0.47	−1.74	−0.72	−0.66	−0.70	0.26	−1.33	−3.22	0.92	−1.85
15–19	−0.56	−0.36	−3.76	−0.76	−1.99	−0.33	−0.02	−3.29	2.90	0.90	−1.26
20–24	−0.15	−0.54	−0.30	−0.87	−0.81	0.18	0.08	−0.08	6.20	0.52	−0.37
25–29	0.08	−0.41	−0.91	−0.19	−0.08	0.29	0.30	1.00	7.85	0.27	−0.81
30–34	−0.01	−0.14	−1.41	−0.35	1.09	0.29	0.23	0.16	7.52	0.16	−2.48
35–39	−0.33	−0.37	−3.81	−0.57	−0.38	0.31	−0.09	−0.32	3.86	0.27	−3.90
40–44	−0.58	−0.54	−5.37	−0.80	0.37	0.25	−0.19	−1.27	1.50	0.35	−3.30
45–49	−0.64	−0.58	−3.48	−0.79	0.86	0.19	−0.17	−0.75	1.72	0.17	−2.08
50–54	−0.58	−0.46	−2.08	−0.45	1.30	0.20	−0.01	0.89	3.65	−0.15	−0.38
55–59	−0.67	−0.46	−2.19	−0.27	1.46	0.17	0.16	0.04	4.94	−0.27	1.16
60–64	−0.83	−0.74	−2.85	−0.39	1.61	0.07	−0.08	−0.82	4.29	−0.15	1.23
65–69	−1.05	−1.05	−2.67	−0.66	1.32	−0.13	−0.24	−1.40	1.74	−0.05	0.25
70–74	−1.18	−1.22	−2.33	−0.72	1.35	−0.22	−0.41	−1.35	0.57	0.04	−0.27
75–79	−1.19	−1.34	−1.88	−0.70	1.41	−0.25	−0.55	−1.32	0.51	0.11	−0.50
80–84	−1.20	−1.55	−1.43	−0.77	1.38	−0.30	−0.70	−1.45	−0.35	0.08	−0.94
85–89	−1.12	−1.73	−1.24	−0.85	1.44	−0.32	−0.76	−1.59	−0.72	0.10	−1.33
90–94	−0.85	−1.55	−0.98	−0.66	1.77	−0.09	−0.76	−1.14	−2.90	0.00	−1.29
95+	−0.62	−1.21	−0.81	−0.58	2.20	0.15	−0.68	−0.47	−6.07	−0.20	−1.22

Table 19

BY-CAUSE MODEL TREND BY AGE ($\beta_x \times 100 \times \Delta$), FEMALE

	Cardio.	Cerebro.	NeoSmok	Neoplasm	Dementia	Diabetes	Influenza	Resp.	Drug	External	Other
0	−1.47	0.29	4.04	−0.68	−1.65	−1.46	−0.01	−0.12	−5.83	−0.03	−1.29
1–4	−0.46	−0.97	−10.73	−0.59	−2.22	−0.92	−0.00	0.59	−1.27	0.10	−1.48
5–9	−0.73	1.16	1.68	−0.67	−2.46	−0.61	0.00	1.21	−3.12	0.18	−1.27
10–14	−1.26	−0.16	−1.86	−0.35	−1.39	−1.03	0.00	0.25	−1.60	0.14	−1.67
15–19	−1.04	−0.33	−3.55	−0.67	−1.46	−0.64	−0.00	−1.78	4.51	0.17	−1.55
20–24	−0.81	−1.21	−1.43	−0.77	−1.46	−0.30	0.00	−1.50	8.85	0.06	−0.93
25–29	−0.35	−0.68	0.84	−0.64	0.95	0.03	0.00	−1.02	10.61	0.02	−1.00
30–34	−0.17	−0.62	−2.20	−0.51	0.09	0.12	0.00	−0.90	9.07	0.03	−1.03
35–39	−0.38	−1.09	−4.51	−0.66	0.99	0.16	0.00	−0.18	5.23	0.07	−1.38
40–44	−0.52	−1.14	−3.94	−0.64	0.54	0.13	0.00	−0.76	3.93	0.06	−1.47
45–49	−0.43	−0.96	−1.80	−0.67	1.08	0.12	0.00	0.90	5.42	0.01	−0.45
50–54	−0.54	−0.63	−0.48	−0.61	1.66	−0.01	0.00	1.71	7.98	−0.03	0.52
55–59	−0.96	−0.90	−1.35	−0.66	1.47	−0.21	0.00	0.47	7.86	−0.04	0.83
60–64	−1.40	−1.13	−2.42	−0.66	1.57	−0.41	−0.00	−0.89	5.48	0.00	0.41
65–69	−1.64	−1.34	−1.72	−0.69	1.31	−0.63	−0.00	−0.68	2.97	0.02	0.15
70–74	−1.68	−1.44	−1.04	−0.64	1.40	−0.54	−0.00	−0.19	0.79	0.02	−0.19
75–79	−1.65	−1.44	−0.48	−0.57	1.53	−0.51	−0.00	0.03	−0.21	0.00	−0.38
80–84	−1.67	−1.59	0.00	−0.59	1.51	−0.45	−0.00	0.14	−0.78	−0.01	−1.04
85–89	−1.61	−1.67	0.33	−0.59	1.57	−0.39	−0.01	0.21	−1.71	−0.03	−1.60
90–94	−1.39	−1.55	0.51	−0.47	1.73	−0.24	−0.01	0.64	−1.33	−0.05	−1.84
95+	−1.20	−1.39	0.96	−0.39	2.02	−0.01	−0.01	0.88	−1.57	−0.09	−1.89

We observe the most negative values for cause NeoSmok (male especially), then cardiovascular and cerebrovascular. We observe the higher values for drug in middle ages and dementia in old ages. Shown below is the quantity $\beta_x \times \sigma$ by age and cause of death, which corresponds to the volatility by age and cause, or the relative yearly standard deviation of stochastic mortality rates (log base).

Table 20

BY-CAUSE MODEL TREND BY AGE ($\beta_x \times 100 \times \sigma$), MALE

	Cardio.	Cerebro.	NeoSmok	Neoplasm	Dementia	Diabetes	Influenza	Resp.	Drug	External	Other
0	0.97	0.23	0.80	0.59	−3.13	5.50	3.77	0.97	−7.18	−1.28	1.23
1–4	0.45	−0.03	9.29	0.99	−3.77	4.15	1.25	−1.40	−0.31	2.16	1.75
5–9	1.02	−0.31	0.80	0.68	−1.71	4.49	−1.83	−4.55	−1.75	5.03	0.69
10–14	1.37	−0.59	1.17	0.91	−1.43	3.21	−2.01	2.48	−2.13	4.61	1.62
15–19	0.76	0.45	2.52	0.96	−4.27	1.50	0.12	6.12	1.92	4.51	1.10
20–24	0.21	0.68	0.20	1.10	−1.75	−0.81	−0.58	0.15	4.11	2.61	0.32
25–29	−0.11	0.51	0.61	0.24	−0.16	−1.33	−2.32	−1.86	5.21	1.36	0.71
30–34	0.01	0.18	0.95	0.44	2.35	−1.33	−1.78	−0.30	4.99	0.79	2.18
35–39	0.44	0.46	2.55	0.72	−0.83	−1.44	0.71	0.59	2.56	1.35	3.42
40–44	0.79	0.67	3.60	1.01	0.80	−1.15	1.46	2.37	0.99	1.74	2.89
45–49	0.86	0.72	2.33	1.00	1.86	−0.87	1.33	1.38	1.14	0.86	1.83
50–54	0.78	0.57	1.39	0.56	2.79	−0.90	0.10	−1.65	2.42	−0.73	0.33
55–59	0.90	0.57	1.46	0.34	3.14	−0.78	−1.21	−0.08	3.28	−1.37	−1.01
60–64	1.12	0.92	1.91	0.49	3.45	−0.33	0.60	1.52	2.84	−0.74	−1.08
65–69	1.41	1.30	1.79	0.83	2.83	0.59	1.82	2.60	1.15	−0.24	−0.22
70–74	1.60	1.52	1.56	0.90	2.90	1.01	3.12	2.51	0.38	0.21	0.23
75–79	1.60	1.67	1.26	0.88	3.02	1.16	4.18	2.45	0.34	0.54	0.44
80–84	1.62	1.93	0.96	0.96	2.96	1.36	5.35	2.70	−0.23	0.38	0.82
85–89	1.50	2.16	0.83	1.07	3.08	1.48	5.84	2.95	−0.48	0.51	1.16
90–94	1.14	1.93	0.66	0.83	3.81	0.41	5.78	2.11	−1.92	0.01	1.13
95+	0.84	1.51	0.54	0.72	4.72	−0.68	5.16	0.87	−4.03	−0.99	1.07

Table 21

BY-CAUSE MODEL TREND BY AGE ($\beta_x \times 100 \times \sigma$), FEMALE

	Cardio.	Cerebro.	NeoSmok	Neoplasm	Dementia	Diabetes	Influenza	Resp.	Drug	External	Other
0	1.62	−0.38	−3.86	0.80	−3.63	6.28	6.70	0.26	−2.33	−0.67	1.28
1–4	0.50	1.27	10.27	0.70	−4.90	3.98	2.19	−1.24	−0.51	2.04	1.47
5–9	0.80	−1.52	−1.61	0.79	−5.41	2.62	−2.67	−2.55	−1.25	3.76	1.26
10–14	1.38	0.22	1.78	0.41	−3.06	4.45	−1.26	−0.53	−0.64	2.87	1.65
15–19	1.14	0.44	3.40	0.78	−3.20	2.77	0.13	3.78	1.81	3.56	1.53
20–24	0.89	1.58	1.36	0.90	−3.21	1.29	−0.76	3.18	3.54	1.23	0.92
25–29	0.39	0.90	−0.80	0.75	2.08	−0.11	−4.78	2.17	4.24	0.52	0.99
30–34	0.19	0.82	2.11	0.60	0.19	−0.52	−3.87	1.90	3.63	0.61	1.02
35–39	0.42	1.43	4.32	0.77	2.18	−0.71	−0.05	0.38	2.09	1.41	1.37
40–44	0.57	1.50	3.78	0.75	1.18	−0.56	−0.76	1.61	1.57	1.25	1.46
45–49	0.47	1.26	1.72	0.79	2.38	−0.52	−0.67	−1.91	2.17	0.19	0.44
50–54	0.59	0.83	0.46	0.72	3.65	0.06	−2.26	−3.61	3.19	−0.69	−0.51
55–59	1.06	1.18	1.29	0.77	3.24	0.92	−1.49	−1.00	3.15	−0.93	−0.82
60–64	1.54	1.48	2.32	0.78	3.45	1.76	0.65	1.89	2.19	0.05	−0.40
65–69	1.80	1.75	1.65	0.81	2.89	2.71	1.31	1.43	1.19	0.38	−0.15
70–74	1.85	1.89	0.99	0.75	3.09	2.33	3.21	0.40	0.32	0.48	0.19
75–79	1.82	1.88	0.46	0.67	3.36	2.19	4.58	−0.05	−0.08	0.10	0.38
80–84	1.84	2.09	−0.00	0.70	3.33	1.95	6.23	−0.29	−0.31	−0.26	1.03
85–89	1.77	2.19	−0.31	0.69	3.47	1.68	7.41	−0.44	−0.69	−0.65	1.59
90–94	1.54	2.03	−0.49	0.55	3.81	1.04	7.59	−1.36	−0.53	−1.13	1.83
95+	1.32	1.83	−0.92	0.45	4.44	0.03	7.44	−1.87	−0.63	−1.84	1.87

The volatility is the highest for influenza, respiratory and dementia. The volatility is the lowest for NeoSmok, neoplasms and external.

5. WHY BY CAUSE PROJECTION IS MORE PESSIMISTIC?

The by-cause forecasts are more pessimistic mainly because the one cause with the higher historical increase (or smaller decrease if all causes are decreasing) will drive the aggregated mortality at some point of the projection. This feature of cause-based models has been studied by Wilmoth (1995). For illustration, consider this example with artificial data. For the sake of simplicity, the age dependency is omitted, there are two causes of death and 10 years of historical data. Moreover, the volatility of the forecasted rates are ignored. Thus, the Lee-Carter model central mortality forecast formula is:

$$\mu_t = \mu_0 \times e^{(\kappa_t - \kappa_0)} = \mu_0 \times e^{\Delta \times t}$$

Suppose that the number of deaths by cause is given in Table 22:

Table 22

NUMBER OF DEATHS–BY CAUSE PROJECTIONS

Year	Cause A	Cause B	Total
2007	70	30	100
2017	50	50	100

Then, the calibration of the by-cause model gives:

- $\Delta_A = \frac{\log(50) - \log(70)}{10} \approx -\mathbf{3.4\%}$
- $\Delta_B = \frac{\log(50) - \log(30)}{10} \approx +\mathbf{5.1\%}$

The trend of the all-causes projection model is: $\Delta = \frac{\log(100) - \log(100)}{10} = \mathbf{0\%}$

The forecasts are illustrated in Table 23.

Table 23

FORECASTS–COMPARISON BY CAUSE VS ALL-CAUSES PROJECTIONS

Year	By cause projections			All-causes projection
	Cause A	Cause B	Total	Total
2017	50	50	100	100
2018	48.3	52.6	101.0	100
2027	35.7	83.3	119.0	100

In this example, the all-causes projection will remain constant while the by-cause projection will have an asymptotic relative variation of +5.1% per year.

From a theoretical view, the ratio between by-cause and all-causes projection is:

$$M_t = \frac{\sum_{i=1}^{n} \mu_0^i \times e^{\Delta^i \times t}}{\mu_0 \times e^{\Delta \times t}} = \sum_{i=1}^{n} p_0^i \times \left(e^{\Delta^i - \Delta}\right)^t$$

p_0^i is the initial proportion of deaths induced by cause i (at time 0).

Wilmoth (1995) has shown two important results to explain the pessimism of by-cause projections.

Theorem 1: M_t is higher than 1 for all value of $t > 0$ if and only if the following inequality holds:

$$\sum_{i=1}^{n} p_0^i \times (\Delta^i - \Delta) > 0$$

If it holds, then M_t is strictly increasing.

Theorem 2: For the classical calibration of the trend (the trend equals the average historical increments), M_t is always higher than 1 (and increasing with t).

When including the age dependency and volatility, the result is not obvious but it is still suspected that the pessimism of the by-cause forecasts is, at least partly, induced by the model. Theorem 1 gives an easy formula for comparison of a by-cause model with an all-cause projection when knowing the improvement rates of the models.

6. CORRECTION OF THE AGGREGATION BIAS WITHIN ALL-CAUSES MORTALITY

Several actual research papers show that a non-negligible part of the mortality rates evolution may be due to age-aggregation bias.

- *Rising morbidity and mortality in midlife among white non-Hispanic Americans in the 21st century.* Anne Case and Agus Deaton.
  The authors find that the mortality increases for white Americans aged 45–54 between 1999 and 2013 by 0.5% per year.

- *Age-aggregation bias in mortality trends.* Andrew Gelmana and Jonathan Auerbacha
  In a letter, the two authors demonstrate that the average age of the group studied raises by 0.4 years during the period and show corrected rates dividing the apparent mortality increase into two terms, the first being induced by the aging of the group, the second being the residual increase in mortality. In conclusion, they state that the increase in mortality is 50% explained by the aging within the 10 years age bands and is mainly observed for women.

Previous work on deaths by cause has always aggregated the rates by age. Groups of five-years in length seem to be a common method and correspond to the data that HCD furnished.

To measure the magnitude of the aggregation bias within rates by cause, the authors assessed the impacts of aggregation on the overall mortality with HMD data.

Figure 25 shows the evolution of the average age of a group.

Figure 25
EVOLUTION OF THE AVERAGE AGE OF A GROUP

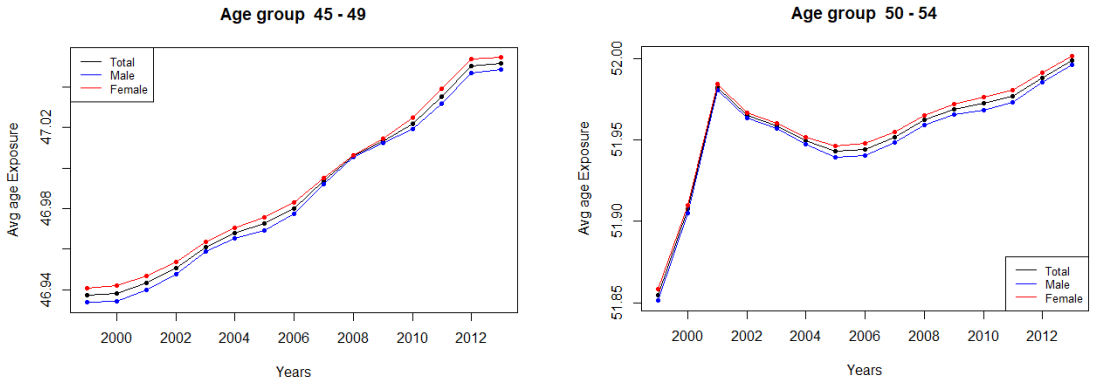

The evolution of the population pyramid between 2009 and 2010 and between 2012 and 2013 shows important irregularities of exposure through generations (see Figure 26). The most important change is caused by the aging of the baby boomer generation.

Figure 26
EVOLUTION OF THE POPULATION PYRAMID

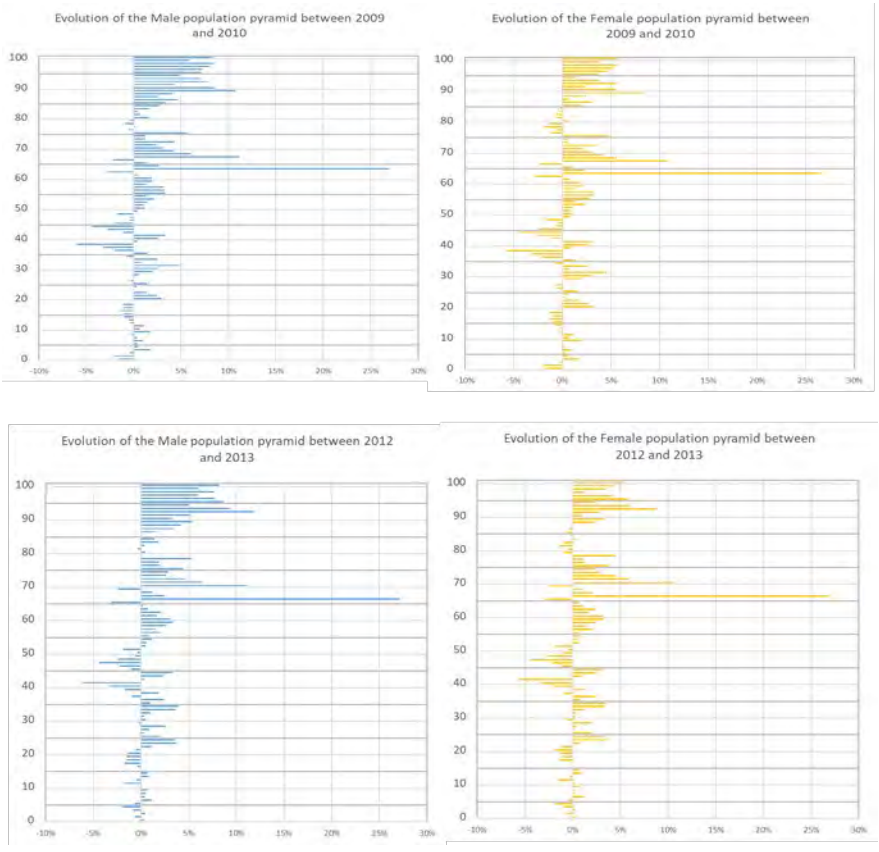

Correction. For each group and gender, the authors assessed the change in percentage of the historical maximum variation induced by the corrected rates (see Figure 27). The impact of correction is not as

important as in the previous papers which focused on 10-year age bands (it was closer to 50%), but the correction is significant for the groups 45–49 years (especially women) and 50–54 years.

Figure 27

RELATIVE IMPACT OF THE AGE-BIAS CORRECTION IN THE HISTORICAL DEVIATION OF THE DEATH RATES

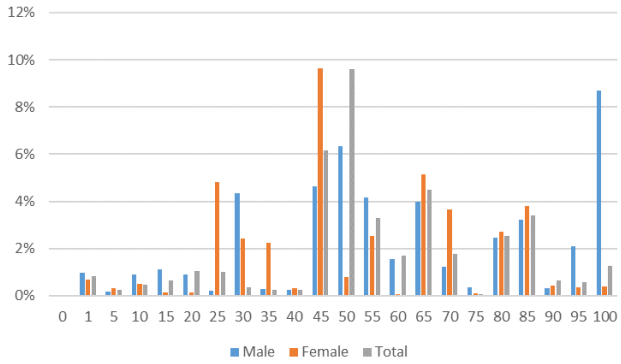

Figure 28 displays the crude and corrected improvement rates for several groups.

Figure 28

CRUDE AND CORRECTED IMPROVEMENT RATES FOR SEVERAL GROUPS

Overall, the age-bias is not as material for five-years age groups as in ten-year age groups. However, as illustrated in these graphs, the estimated improvements may still differ by several percentages. Depending on the cause-of-death and age group focus, it may be of interest to deploy this methodology. In this report, however, the authors preferred to use crude HCD data to ensure appropriate reproducibility of the forecasting results by other parties.

7. COMPARISON BETWEEN A BY-CAUSE MODEL AND AN ALL-CAUSES MODEL

The aim of this section is to perform the comparison between the by-cause and all-causes forecasts using breakpoint detection for both models. The breakpoint year of the all-causes model is fixed at 2009 for both males and females.

Figures 29–30 plot the life expectancy central projections using the Lee-Carter model for a by-cause projection and for an all-causes projection.

Figure 29

COMPARISON OF THE ALL-CAUSES AND THE BY-CAUSE MODEL–LIFE EXPECTANCY AT BIRTH

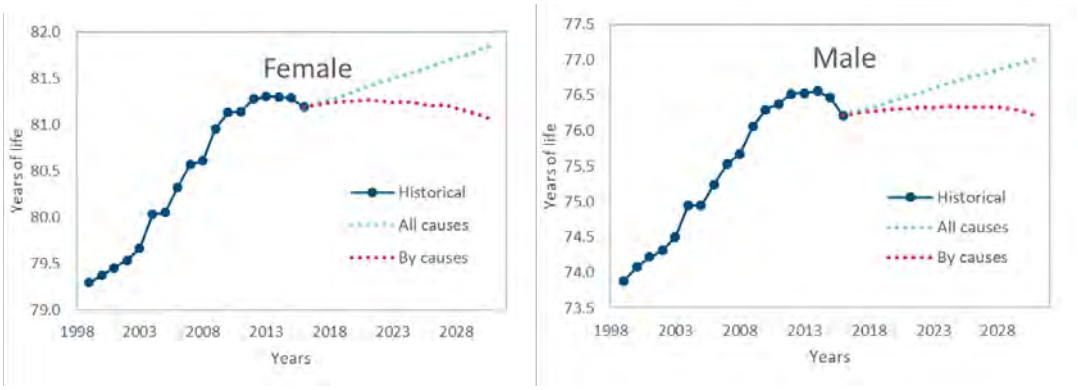

Figure 30

COMPARISON OF THE ALL-CAUSES AND THE BY-CAUSE MODEL–LIFE EXPECTANCY AT 60 YEARS OLD

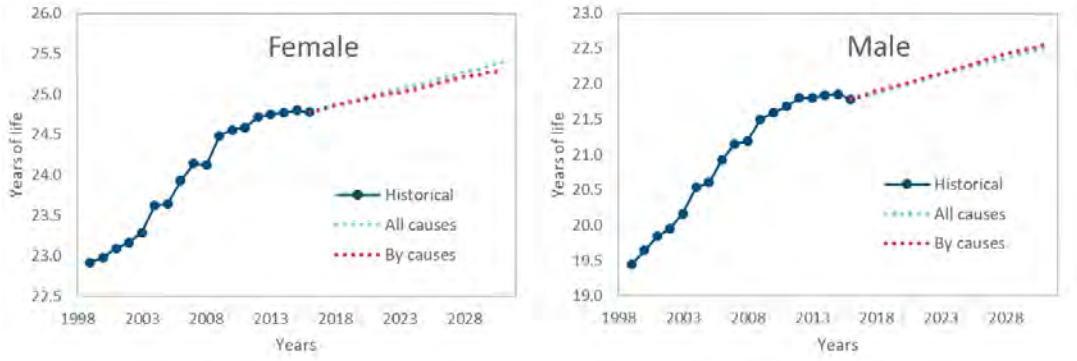

Again, the cause-based forecast is still more pessimistic on the general life expectancy. This is explained by the projected increase in drug causes at young ages. However, for the life expectancy at 60 years, the two models provide comparable central forecasts. This stability phenomenon on life expectancy at 60 years is of particular interest because it shows that the two models agree, even though there are very different in terms of underlying data and model specification. This may be seen as a good argument for the classical Lee-Carter model to be used to forecast mortality at higher ages than usually considered (starting at age zero), in contexts where underlying causes of death do not show major fluctuations.

The average projected yearly life expectancy improvements at ages 0, 40, 60 and 80 (in months) are given in the Tables 24 and 25.

Table 24

AVERAGE YEARLY IMPROVEMENT IN LIFE EXPECTANCY FOR BY-CAUSE OR ALL-CAUSES FORECASTS, FEMALE

	0	40	60	80
By-cause	−0.1	0.2	0.4	0.2
All-causes	0.5	0.5	0.5	0.3

Table 25

AVERAGE YEARLY IMPROVEMENT IN LIFE EXPECTANCY FOR BY-CAUSE OR ALL-CAUSES FORECASTS, MALE

	0	40	60	80
By-cause	−0.0	0.5	0.6	0.3
All-causes	0.6	0.6	0.6	0.4

References

Alai, Daniel H., Séverine, Arnold, Madhavi, Bajekal, and Andrés M., Villegas. 2018. Mind the Gap: A Study of Cause-Specific Mortality by Socioeconomic Circumstances. *North American Actuarial Journal*, 22, no. 2:161-181.

American Cancer Society. 2018. Cancer Facts & Figures 2018. https://www.cancer.org/research/cancer-facts-statistics/all-cancer-facts-figures/cancer-facts-figures-2018.html (accessed on October 17, 2019).

Arnold, Séverine, Alexandre, Boumezoued, Héloïse Labit, Hardy, Nicole, El Karoui. (2018). Cause-of-Death Mortality: What Can Be Learned from Population Dynamics?. *Insurance: Mathematics and Economics*, 78:301-315.

Bergeron-Boucher, Marie-Pier, Vladimir, Canudas-Romo, Jim, Oeppen, and James W., Vaupel. 2017. Coherent Forecasts of Mortality with Compositional Data Analysis. *Demographic Research*, 37:527-566.

Brouhns, Natacha, Michael, Denuit, and Jeroen K, Vermunt. 2002. A Poisson Log-Bilinear Regression Approach to the Construction of Projected Lifetables. *Insurance: Mathematics and economics*, 31, no. 3:373-393.

Cairns, Andrew J.G., David, Blake, Kevin, Dowd, Guy D., Coughlan, David, Epstein, and Marwa, Khalaf-Allah. 2011. Mortality Density Forecasts: An Analysis of Six Stochastic Mortality Models. *Insurance: Mathematics and Economics*, 48, no. 3:355-367.

Cairns, Andrew J., David, Blake, Kevin, Dowd, Guy, Coughlan, David, Epstein, et al. 2009. A Quantitative Comparison of Stochastic Mortality Models Using Data from England and Wales and the United States. *North American Actuarial Journal*, 13, no. 1:1-35.

Canudas-Romo, Vladimir, Eva, DuGoff, Albert W., Wu, Saifuddin, Ahmed, and Gerard, Anderson. 2016. Life Expectancy in 2040: What Do Clinical Experts Expect?. *North American Actuarial Journal*, 20, no. 3:276-285.

Case, A., & Deaton, A. 2016. Reply to Schmid, Snyder, and Gelman and Auerbach: Correlates of the Increase in White Non-Hispanic Midlife Mortality in the 21st century. *Proceedings of the National Academy of Sciences*, 113, no. 7:E818-E819.

Case, Anne, and Angus, Deaton. 2015. Rising Morbidity and Mortality in Midlife Among White Non-Hispanic Americans in the 21st Century. *Proceedings of the National Academy of Sciences*, 112, no. 49:15078-15083.

Caselli, G., Vallin, J., and Marsili, M. 2019. How Useful are the Causes of Death When Extrapolating Mortality Trends. An Update. *Old and New Perspectives on Mortality Forecasting,* 237-259. Switzerland: Springer Open.

Chetty, Raj, Michael, Stepner, Sarah, Abraham, Shelby, Lin, Benjamin, Scuderi, et al. 2016. The Association Between Income and Life Expectancy in the United States, 2001–2014. *JAMA*, 315, no. 16:1750-1766.

Czado, Claudia, Antoine, Delwarde, and Michel, Denuit. 2005. Bayesian Poisson Log-bilinear Mortality Projections. *Insurance: Mathematics and Economics*, 36, no. 3:260-284.

Dimitrova, Dimitrina, Steven, Haberman, and Vlademir K., Kaishev. 2013. Dependent Competing Risks: Cause Elimination and Its Impact on Survival. *Insurance: Mathematics and Economics*, 53, no. 2:464-477.

Dowd, Kevin, Andrew J.G., Cairns, David, Blake, Guy, Coughlan, David, Epstein, et al. 2010. Evaluating the Goodness of Fit of Stochastic Mortality Models. *Insurance: Mathematics and Economics*, 47, no. 3:255-265.

Feigin, Valery L., Gregory A., Roth, Mohsen, Naghavi, Priya, Parmar, Rita, Krishnamurthi, et al. 2016. Global Burden of Stroke and Risk Factors in 188 Countries, During 1990–2013: A Systematic Analysis for the Global Burden of Disease Study 2013. *The Lancet Neurology*, 15, no. 9:913-924.

Foreman, Kyle J., Neal, Marquez, Andrew, Dolgert, Kai, Fukutaki, Nancy, Fullman, et al. 2018. Forecasting Life Expectancy, Years of Life Lost, and All-Cause and Cause-Specific Mortality for 250 Causes of Death: Reference and Alternative Scenarios for 2016–40 for 195 Countries and Territories. *The Lancet*, 392, no. 10159:2052-2090.

Gelman, Andrew, and Jonathan, Auerbach. 2016. Age-Aggregation Bias in Mortality Trends. *Proceedings of the National Academy of Sciences*, 113, no. 7:E816-E817.

Glushko, Viktoriya, and Séverine, Arnold. 2018. Common Factor Decomposition of Cause-Specific Mortality Rates Using the Cointegration Analysis. Presented at the Longevity 14 Conference, Amsterdam, September 2018.

Human Cause-of-Death Database. French Institute for Demographic Studies (France) and Max Planck Institute for Demographic Research (Germany). www.causeofdeath.org (accessed January 2019).

Human Mortality Database. University of California, Berkeley (USA), and Max Planck Institute for Demographic Research (Germany). www.mortality.org or www.humanmortality.de (accessed January 2019).

Institute for Health Metrics and Evaluation (IHME). GBD Results tool. Seattle, WA: IHME, University of Washington, 2017. Available from http://ghdx.healthdata.org/gbd-results-tool (accessed January 2019).

Kjærgaard, Søren, Yunus E., Ergemen, Malene, Kallestrup-Lamb, Jim, Oeppen, and Rune, Lindahl-Jacobsen. 2018. Forecasting Causes of Death Using Compositional Data Analysis: The Case of Cancer Deaths. Presented at the Fourteenth International Longevity Risk and Capital Markets Solutions Conference (Longevity 14), Amsterdam, September 2018.

Koehler, Anne B., Ralph, Snyder, J. Keith, Ord, and Adrian, Beaumont. 2010. Forecasting Compositional Time Series with Exponential Smoothing Methods (No. 20/10). Monash University, Department of Econometrics and Business Statistics.

Lee, Ronald D., and Lawrence, Carter. 1992. Modeling and Forecasting US Mortality. *Journal of the American Statistical Association*, 87, no. 419:659-671.

Li, Han, Hong, Li, Yang, Lu, Y., and Anastasios, Panagiotelis. 2019. A Forecast Reconciliation Approach to Cause-of-Death Mortality Modeling. *Insurance: Mathematics and Economics*, 86, no. 5:122-133

Murray, Christopher J., and Alan, Lopez. 1997. Alternative Projections of Mortality and Disability by Cause 1990–2020: Global Burden of Disease Study. *The Lancet*, 349, no. 9064:1498-1504.

Nelson, Sue, Laurie, Whitsel, Olga, Khavjou, Diane, Phelps, and Alyssa, Leib, A. 2016. Projections of Cardiovascular Disease Prevalence and Costs. RTI International. https://healthmetrics.heart.org/wp-content/uploads/2017/10/Projections-of-Cardiovascular-Disease.pdf (accessed October 17, 2019).

Oeppen, Jim. 2008. Coherent Forecasting of Multiple-Decrement Life Tables: A Test Using Japanese Cause of Death Data. Paper presented at the European Population Conference 2008, July 9–12, 2008, Barcelona, Spain.

Piveteau, Samuel, and Julien, Tomas. 2018. Mortality Forecasting by Cause of Death and Basis Risk Modelling With Compositional Data. Presented at the Longevity 14 Conference, Amsterdam, September 2018.

Priyadarshana, W.J.R.M., and Georgy, Sofronov. 2015. Multiple Break-Points Detection in Array CGH Data Via the Cross-Entropy Method. *IEEE/ACM Transactions on Computational Biology and Bioinformatics*, 12, 2:487-498.

Rahib, L.ola, Benjamin, Smith, Rhonda, Aizenberg, Allison, Rosenzweig, Julie, Fleshman, et al. 2014. Projecting Cancer Incidence and Deaths to 2030: The Unexpected Burden of Thyroid, Liver, and Pancreas Cancers in the United States. *Cancer Research*, 74:11:2913-2921.

Richards, S.J. 2009. Selected Issues in Modelling Mortality by Cause and in Small Populations. *British Actuarial Journal*, 15, no. S1:267-283.

Roth, Gregory, Degu, Abate, Kalkidan, Hassan Abate, Solomon, Abay, Cristiana, Abbafati, et al. 2018. Global, Regional, and National Age-Sex-Specific Mortality for 282 Causes of Death in 195 Countries and Territories, 1980–2017: A Systematic Analysis for the Global Burden of Disease Study 2017. *The Lancet*, 392, no. 10159:1736-1788.

Salhi, Yahia, and Pierre-Emmanuel, Thérond. 2018. Age-Specific Adjustment of Graduated Mortality. *ASTIN Bulletin: The Journal of the IAA*, 48, 2:543-569.

Salhi, Yahia, Pierre-Emmanuel, Thérond, and Julien, Tomas. 2016. A Credibility Approach of the Makeham Mortality Law. *European Actuarial Journal*, 6, no. 1:61-96.

Society of Actuaries. 2019. U.S. Population Mortality Observations – Updated with 2017 Experience. https://www.soa.org/resources/research-reports/2018/population-mortality-observations/ (accessed October 17, 2019).

Sung, Hyuna, Rebecca, Siegel, Phillip, Rosenberg, and Ahmedin, Jemal. 2019. Emerging Cancer Trends Among Young Adults in the USA: Analysis of a Population-Based Cancer Registry. *The Lancet Public Health*, 4: no. 3,137-147

Villegas, Andrés M., Vladimir K. Kaishev, Pietro Millossovich. 2018. StMoMo: An R package for stochastic mortality modeling. Journal of Statistical Software 84(3).

Weir, Hannah K., Trevor, Thompson, Ashwini, Soman, Bjorn, Møller, Steven, Leadbetter, et al. 2015. Peer Reviewed: Meeting the Healthy People 2020 Objectives to Reduce Cancer Mortality. *Preventing Chronic Disease*, 12.

Weir, Hannah K., Robert, Anderson, Sallyann, Coleman King, Ashwini, Soman, Trevor, Thompson, et al. 2016. Peer Reviewed: Heart Disease and Cancer Deaths—Trends and Projections in the United States, 1969–2020. *Preventing Chronic Disease,* 13.

Wilmoth, John R. 1995. Are Mortality Projections Always More Pessimistic When Disaggregated by Cause of Death?. *Mathematical Population Studies*, 5, no. 4:293-319.

World Health Organization. 2004. *International statistical classification of diseases and related health problems (Vol. 1).* World Health Organization, Geneva.

About The Society of Actuaries

The Society of Actuaries (SOA), formed in 1949, is one of the largest actuarial professional organizations in the world dedicated to serving more than 30,000 actuarial members and the public in the United States, Canada and worldwide. In line with the SOA Vision Statement, actuaries act as business leaders who develop and use mathematical models to measure and manage risk in support of financial security for individuals, organizations and the public.

The SOA supports actuaries and advances knowledge through research and education. As part of its work, the SOA seeks to inform public policy development and public understanding through research. The SOA aspires to be a trusted source of objective, data-driven research and analysis with an actuarial perspective for its members, industry, policymakers and the public. This distinct perspective comes from the SOA as an association of actuaries, who have a rigorous formal education and direct experience as practitioners as they perform applied research. The SOA also welcomes the opportunity to partner with other organizations in our work where appropriate.

The SOA has a history of working with public policymakers and regulators in developing historical experience studies and projection techniques as well as individual reports on health care, retirement and other topics. The SOA's research is intended to aid the work of policymakers and regulators and follow certain core principles:

Objectivity: The SOA's research informs and provides analysis that can be relied upon by other individuals or organizations involved in public policy discussions. The SOA does not take advocacy positions or lobby specific policy proposals.

Quality: The SOA aspires to the highest ethical and quality standards in all of its research and analysis. Our research process is overseen by experienced actuaries and nonactuaries from a range of industry sectors and organizations. A rigorous peer-review process ensures the quality and integrity of our work.

Relevance: The SOA provides timely research on public policy issues. Our research advances actuarial knowledge while providing critical insights on key policy issues, and thereby provides value to stakeholders and decision makers.

Quantification: The SOA leverages the diverse skill sets of actuaries to provide research and findings that are driven by the best available data and methods. Actuaries use detailed modeling to analyze financial risk and provide distinct insight and quantification. Further, actuarial standards require transparency and the disclosure of the assumptions and analytic approach underlying the work.

Society of Actuaries
475 N. Martingale Road, Suite 600
Schaumburg, Illinois 60173
www.SOA.org